r-Process Radioisotopes and Their Astrophysical Observables

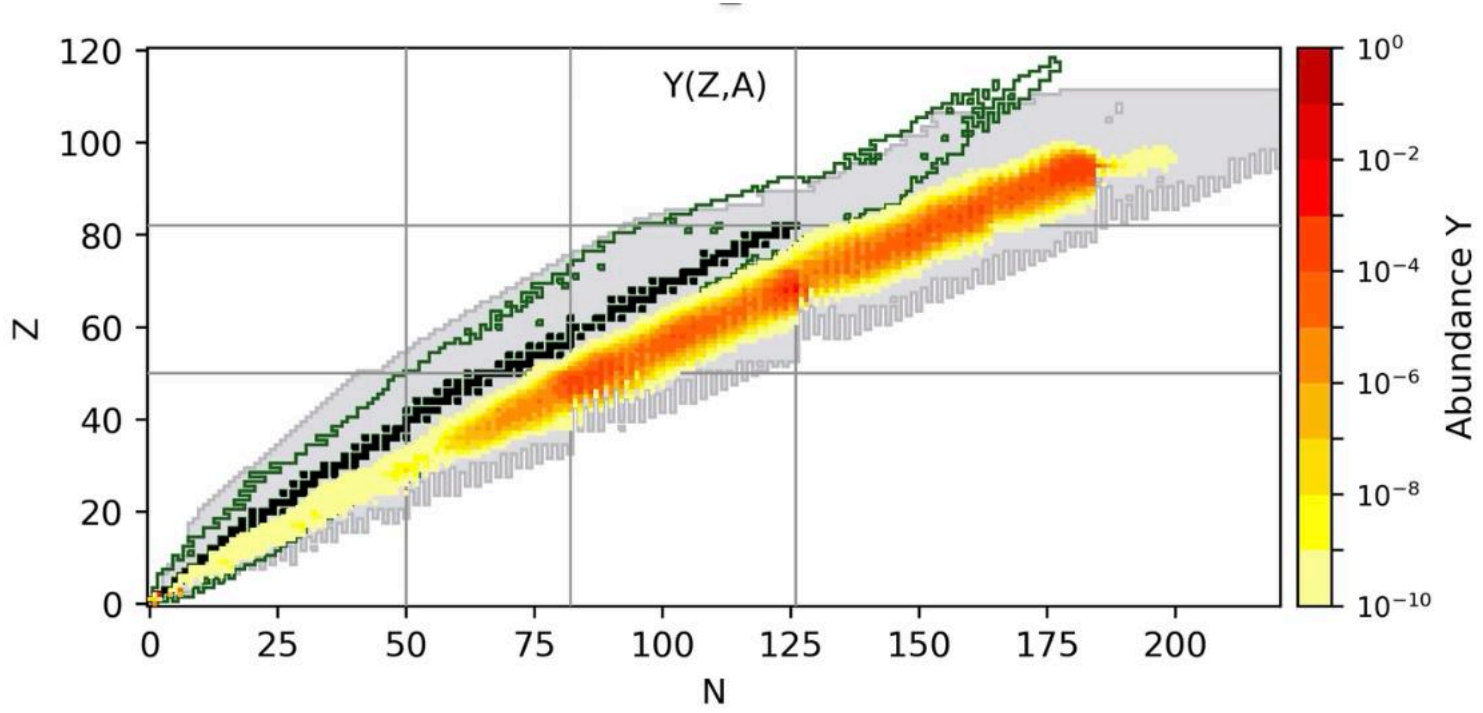
Xilu Wang（王夕露）
wangxl@ihep.ac.cn
Institute of High Energy Physics,
Chinese Academy of Sciences

@ The 6th International Workshop on Origin of Elements and Cosmic Evolution

中国科学院高能物理研究所
Institute of High Energy Physics
Chinese Academy of Sciences

r-process nucleosynthesis

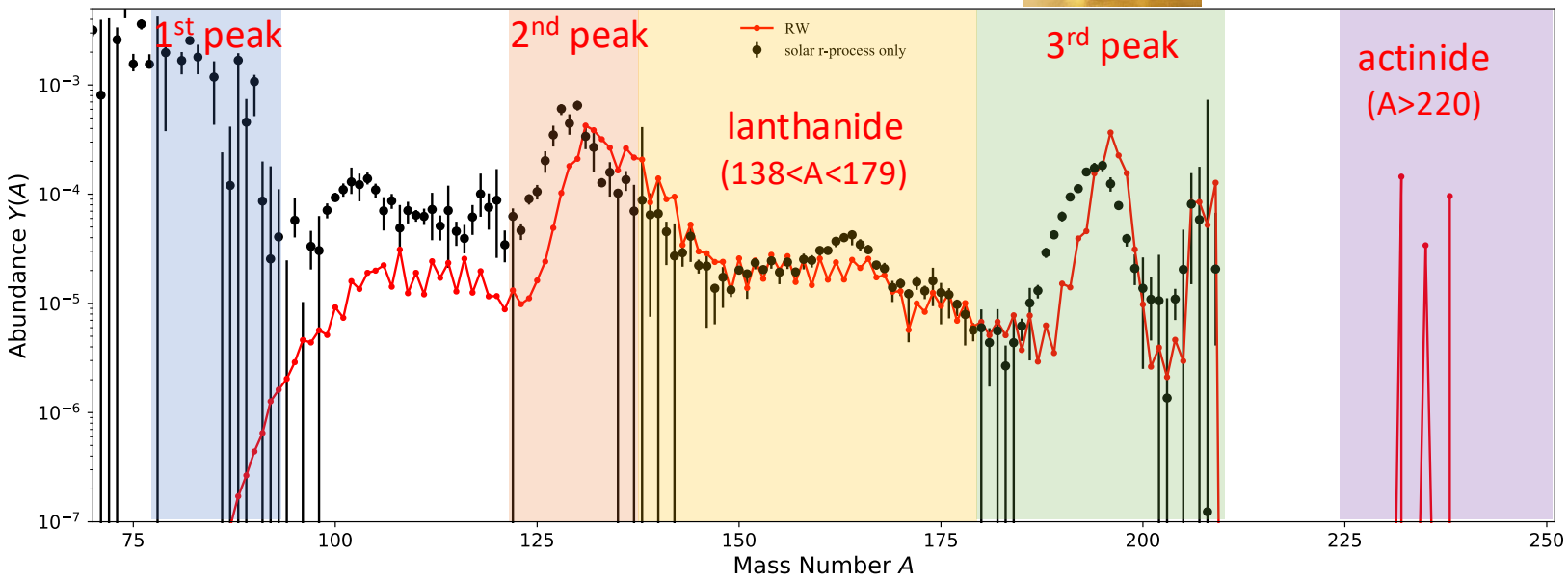
- Rapid neutron-capture process (r process):
  - ✓Create ~half of the nuclei heavier than iron
  - ✓Occurs in neutron-rich environments
  - ✓Abundance peaks: A~82, A~130, A~196 (closed shell structures at N = 50, N = 82, and N = 126)



r-process nucleosynthesis

- Rapid neutron-capture process (r process):
  - ✓Create ~half of the nuclei heavier than iron
  - ✓Occurs in neutron-rich environments
  - ✓Abundance peaks: A~82, A~130, A~196 (closed shell structures at N = 50, N = 82, and N = 126)

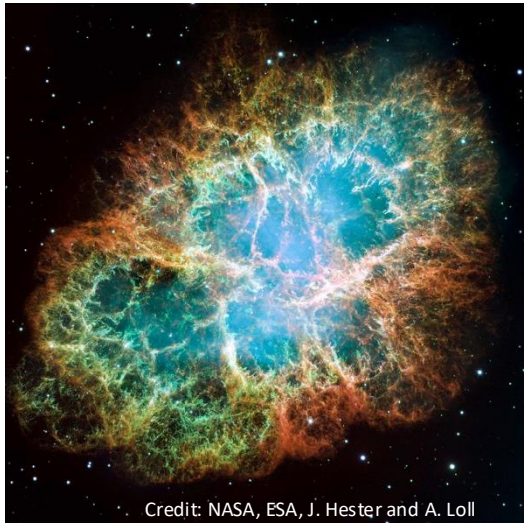




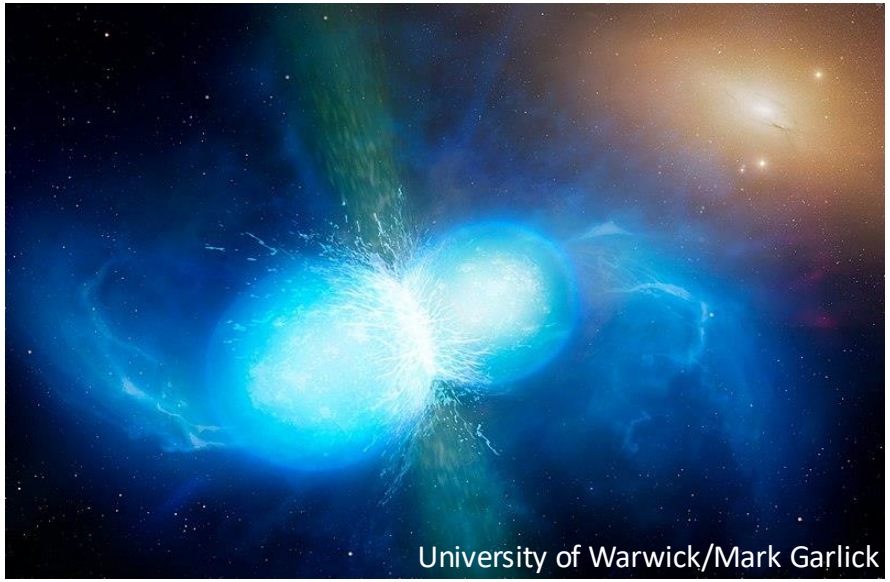
Weak r process: 2nd peak + some lanthanides
Main/Robust r process: 3rd peak, actinides & beyond

r-process sites: a mystery

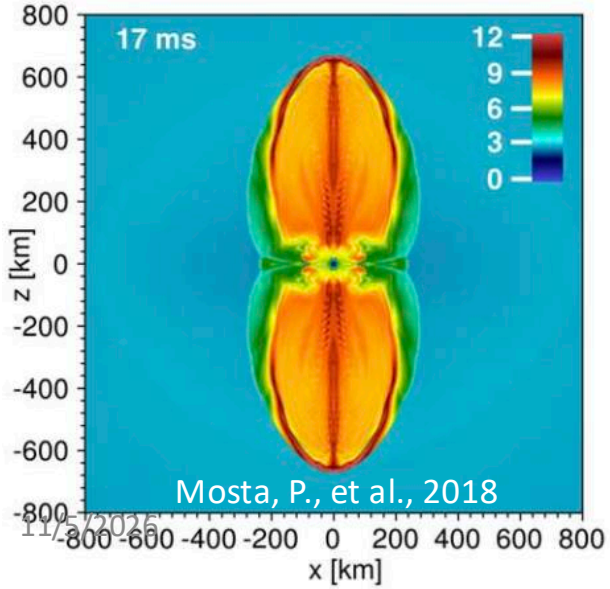
Core collapse Supernovae?
(e.g., Meyer+1992, Roberts+2012)



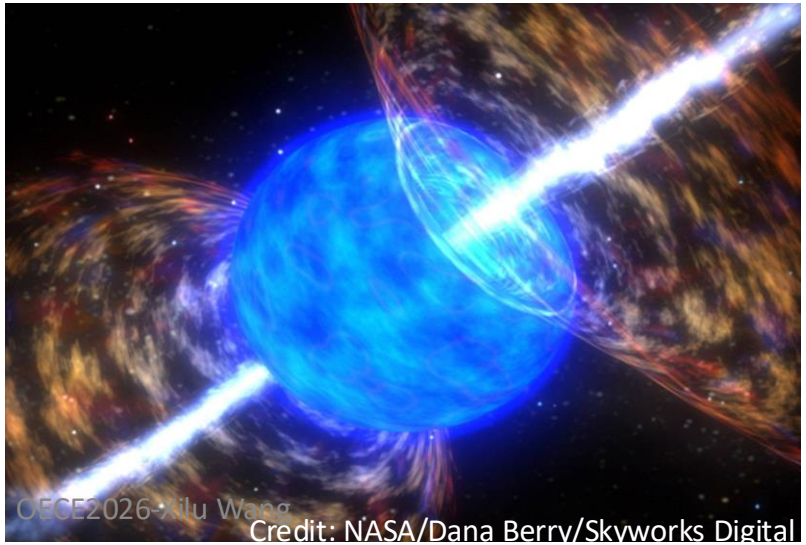
Neutron star + neutron star/black hole mergers
(e,g, Nedora+2020, Foucart+2020, George+2020, etc.)



Magneto-rotational supernovae
(e.g., Reichart+2020, Nishimura+2017, Mosta+2018)



Collapsars
(e.g., Siegel+2019, Miller+2019)



Magnetar giant flare
(e.g., Patel+2025)

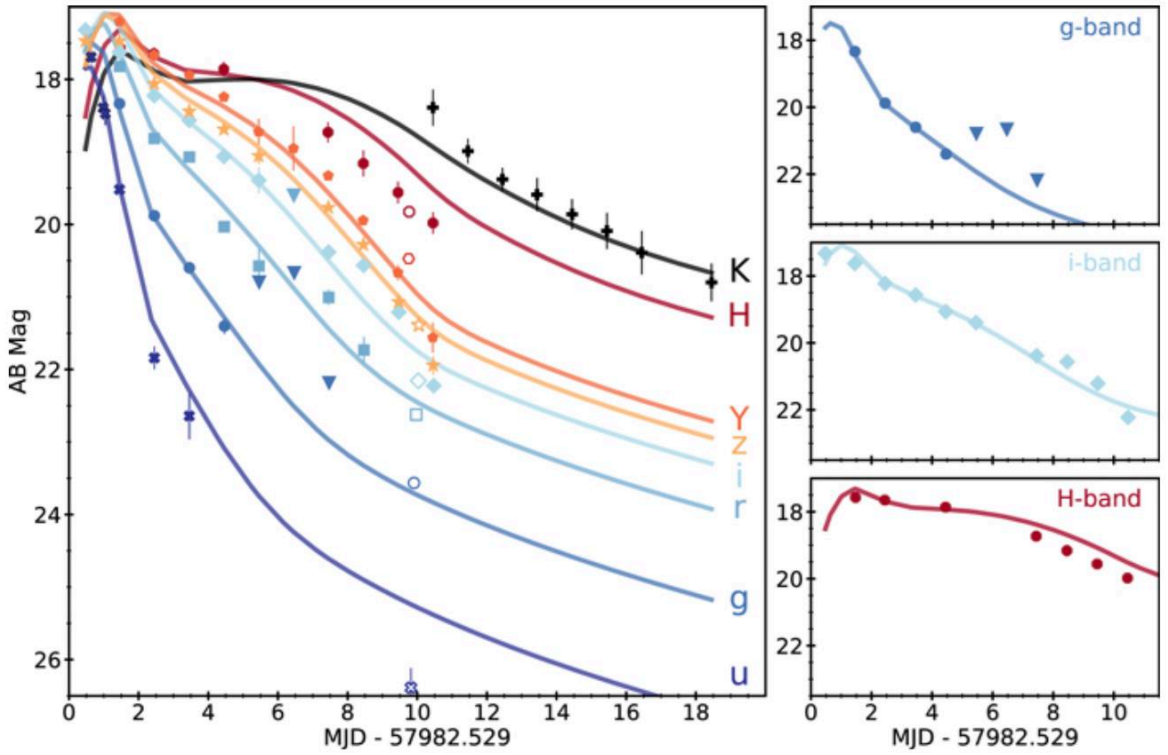
exotic supernovae
(e.g., Fischer+2020)

primordial black hole + neutron star (e.g., Fuller+2017)

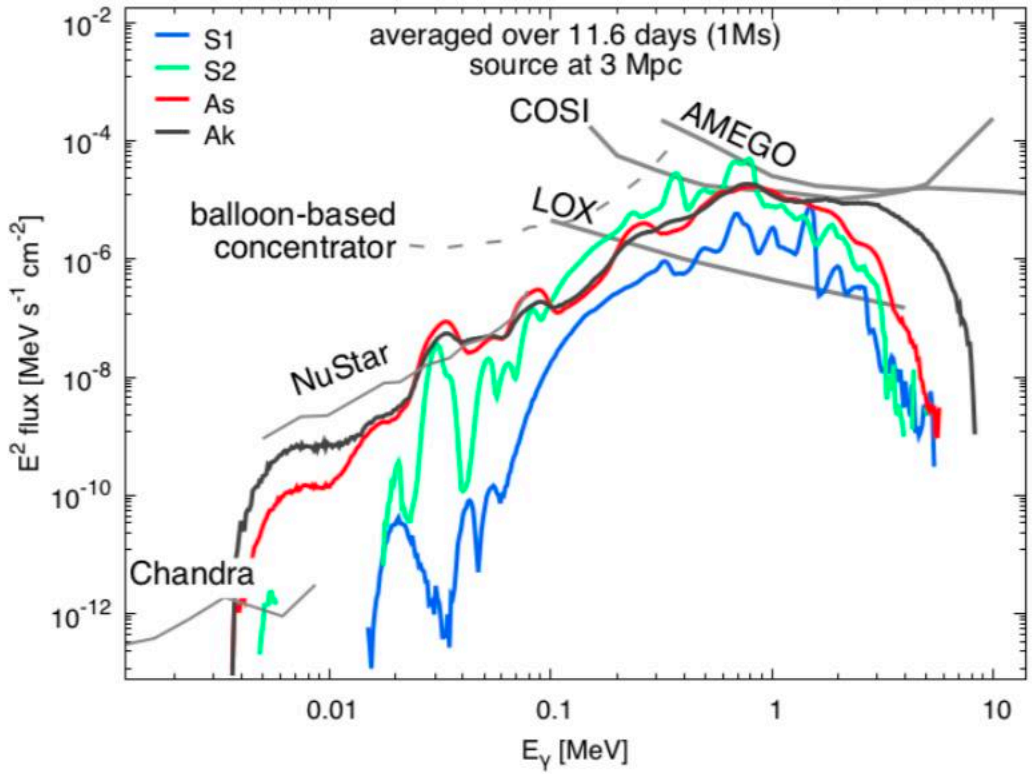
etc.

Astrophysical observables of r-process radioisotopes

- Prompt electromagnetic emissions
  - Kilonova: a transient powered by the radioactive decay of the **r-process isotopes** synthesized from the r-process sites like neutron star merger



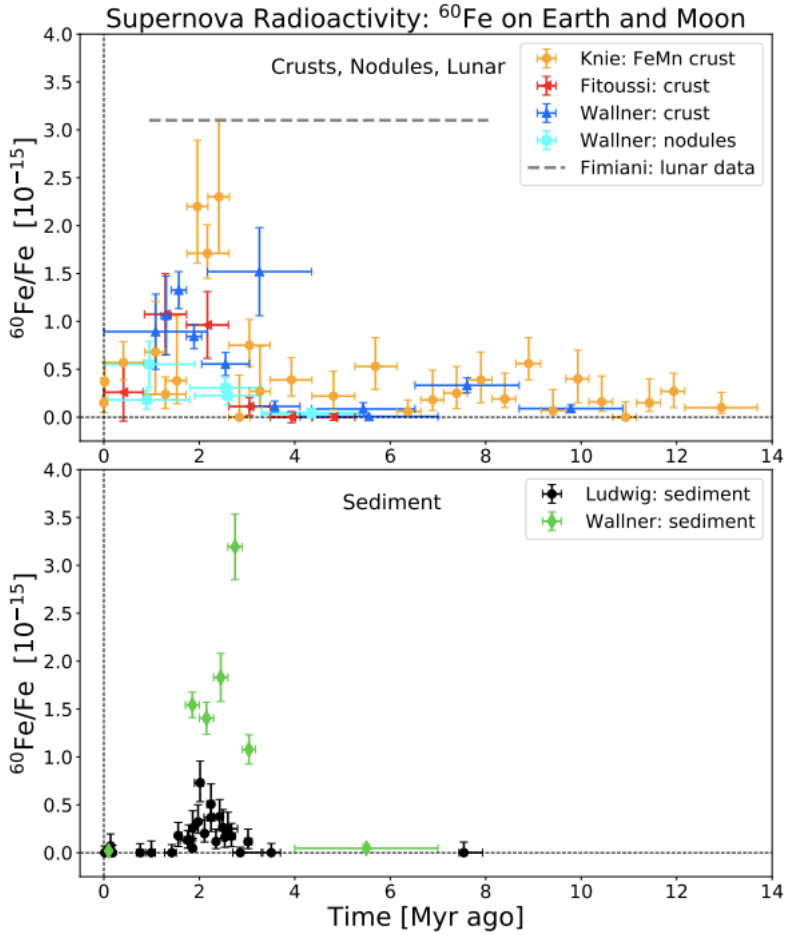
UV, optical, and NIR light curves of the counterpart of GW170817. (Cowperthwaite, P. S., et al., 2017)



Gamma rays from a nearby kilonova. (Korobkin. O., et al., 2020)

Astrophysical observables of r-process radioisotopes

- **isotope** measurements in the solar system samples (Earth, moon, meteorites)



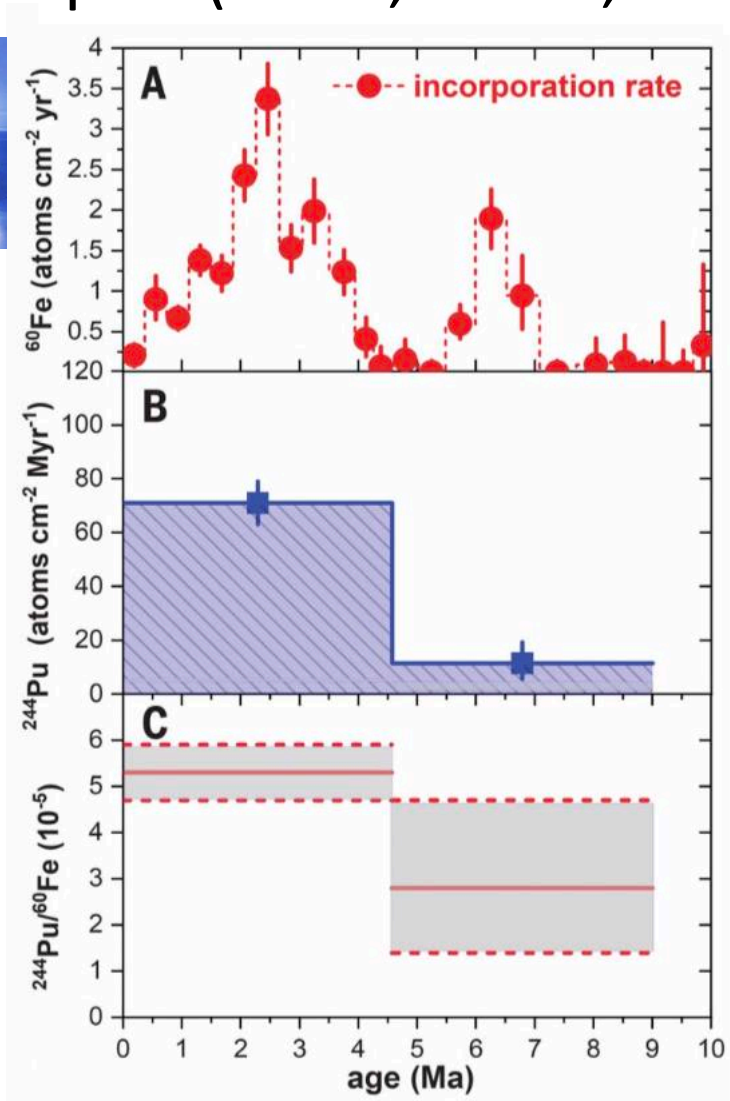
Fields, B., et al. 2019, BAAS, 51,410



$t_{mean,^{60}_{26}Fe} = 3.78\ Myr$

$t_{mean,^{244}_{94}\mathrm{Pu}} = 115\ Myr$

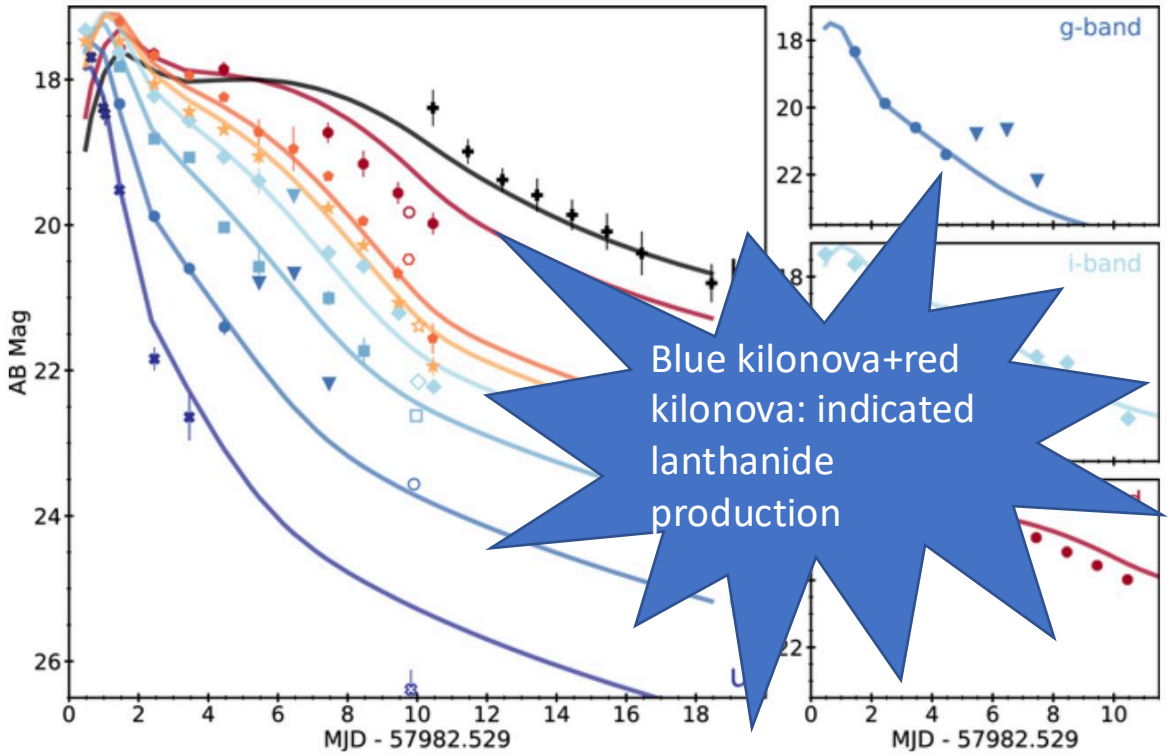
Near-earth event:
within~100pc;
occur ~ 3Myr ago



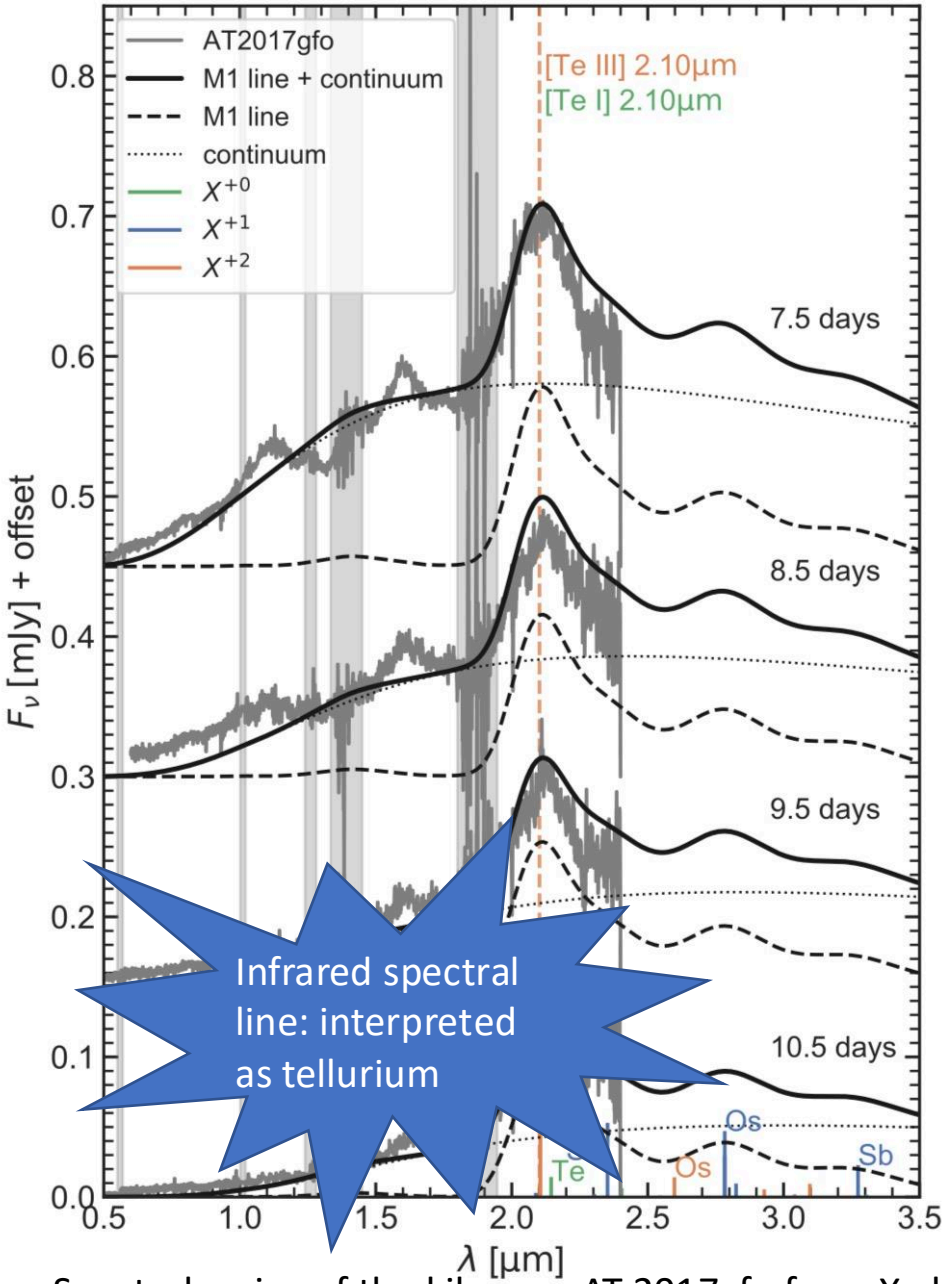
Wallner, A., et al. 2021, Science, 372, 6543

Neutron star mergers (NSM)

- **GW170817**: multi-wavelength observations →confirmed r-process nucleosynthesis sites
  - ➢ Kilonova light curve: Lanthanides production
  - ➢ Strontium and Tellurium elements indicated from spectroscopy
- GRB211211A and GRB230307A: kilonova lightcurve; tellerium

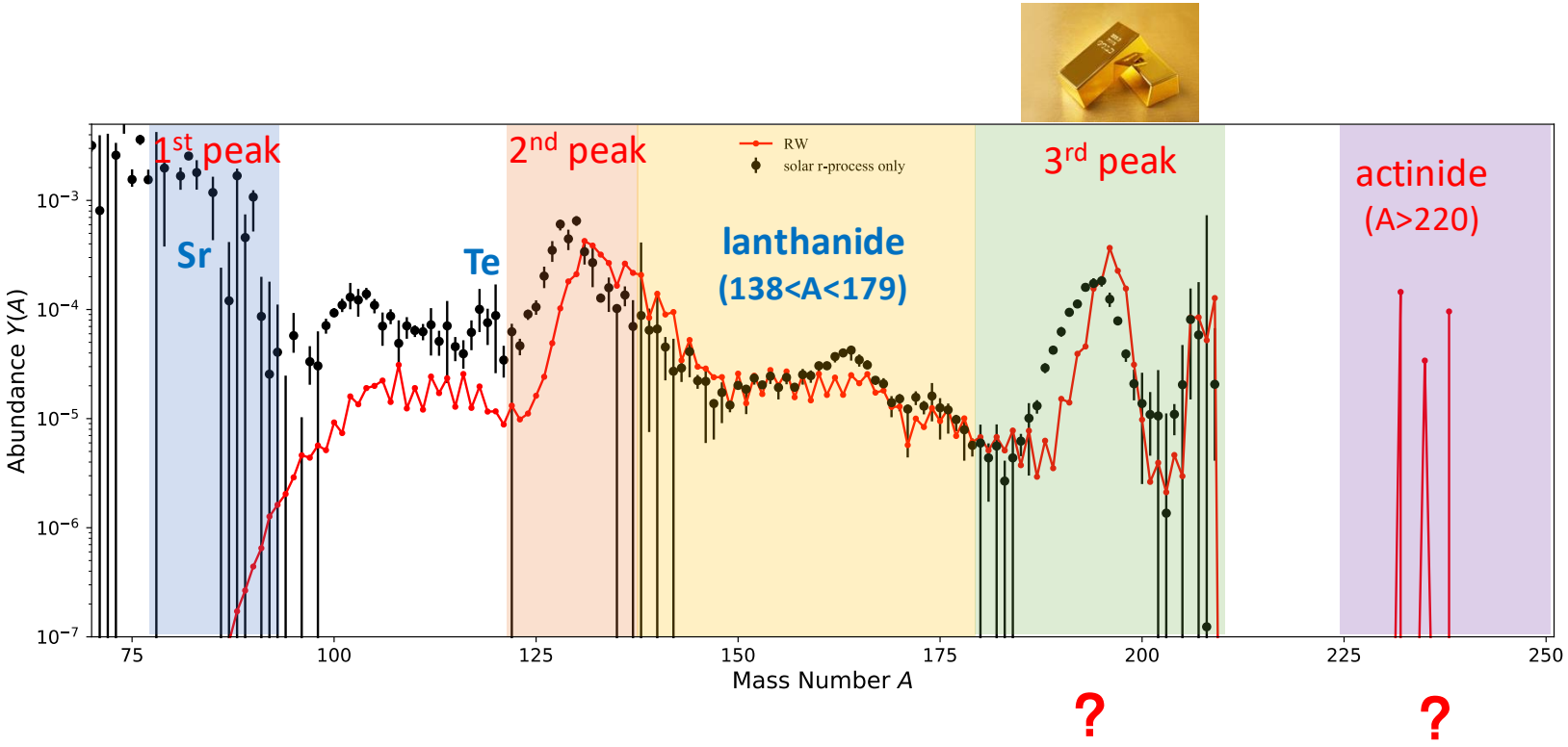


UV, optical, and NIR light curves of the counterpart of GW170817. (Cowperthwaite, P. S., et al., 2017)



Spectral series of the kilonova AT 2017gfo from X-shooter on VLT. (Hotokezaka, K., et al., 2023)

Did the GW170817 merger produce actinides?



Fission in astrophysical environments

Gammas > 3.5 MeV: signature of prompt and delayed **fission gammas** in an astrophysical event!

Incident neutron strikes

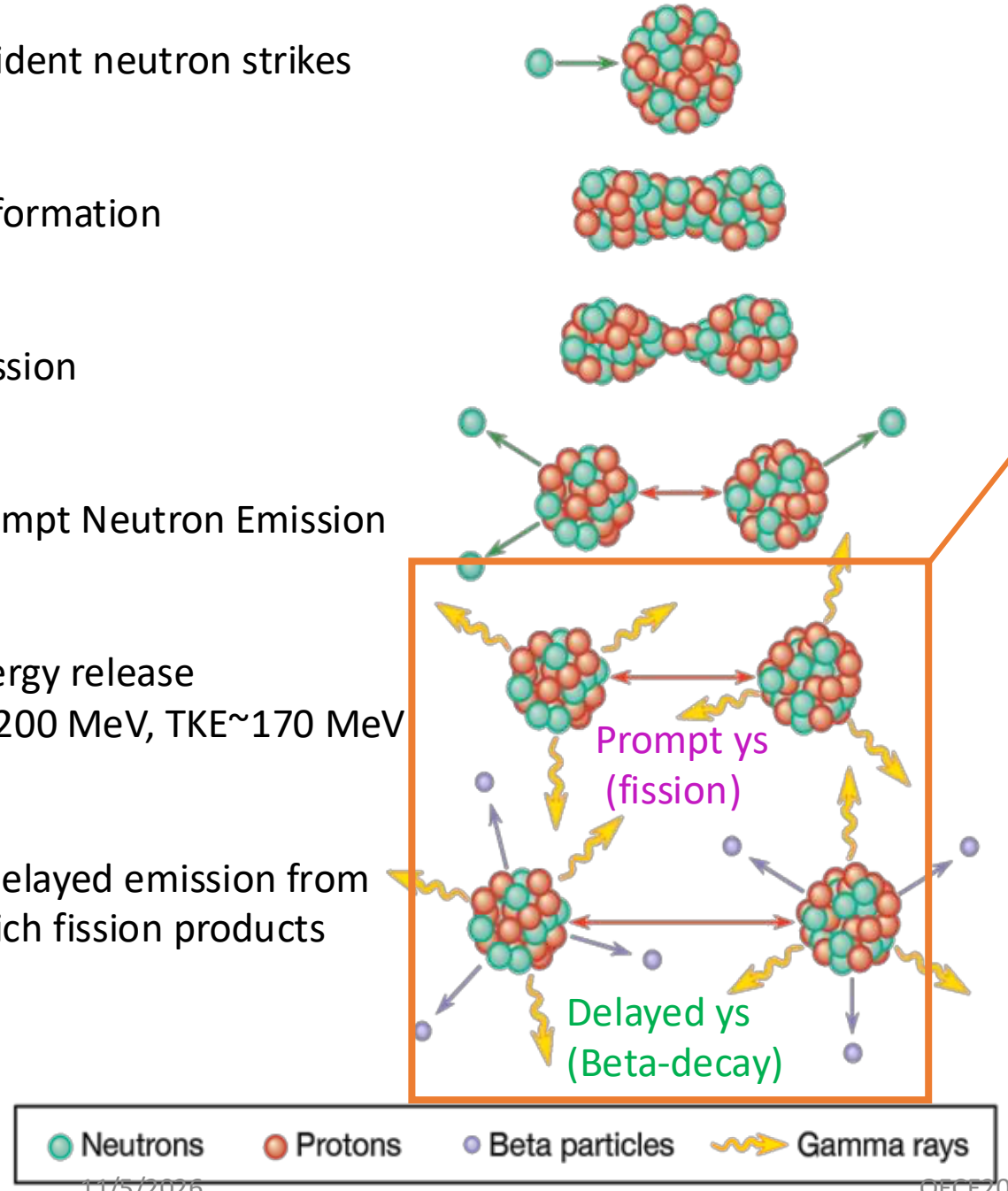
Deformation

Scission

Prompt Neutron Emission

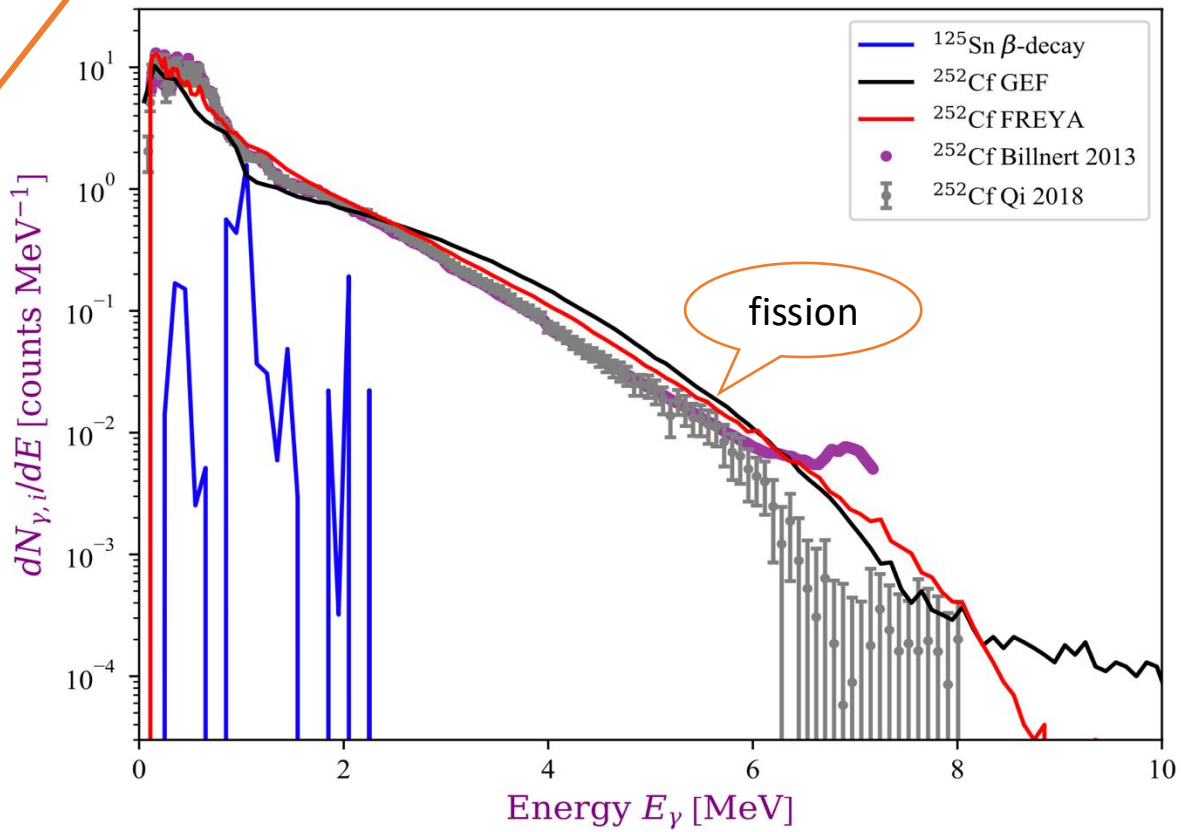
Energy release
Q~200 MeV, TKE~170 MeV

β-delayed emission from
n-rich fission products



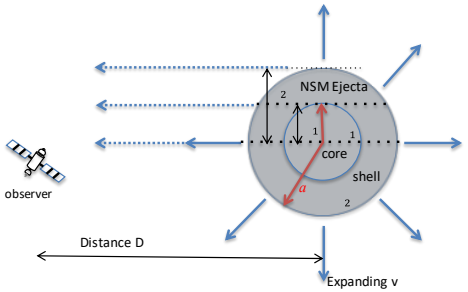
© 2013 Encyclopædia Britannica, Inc.

Credit: Nicole Vassh

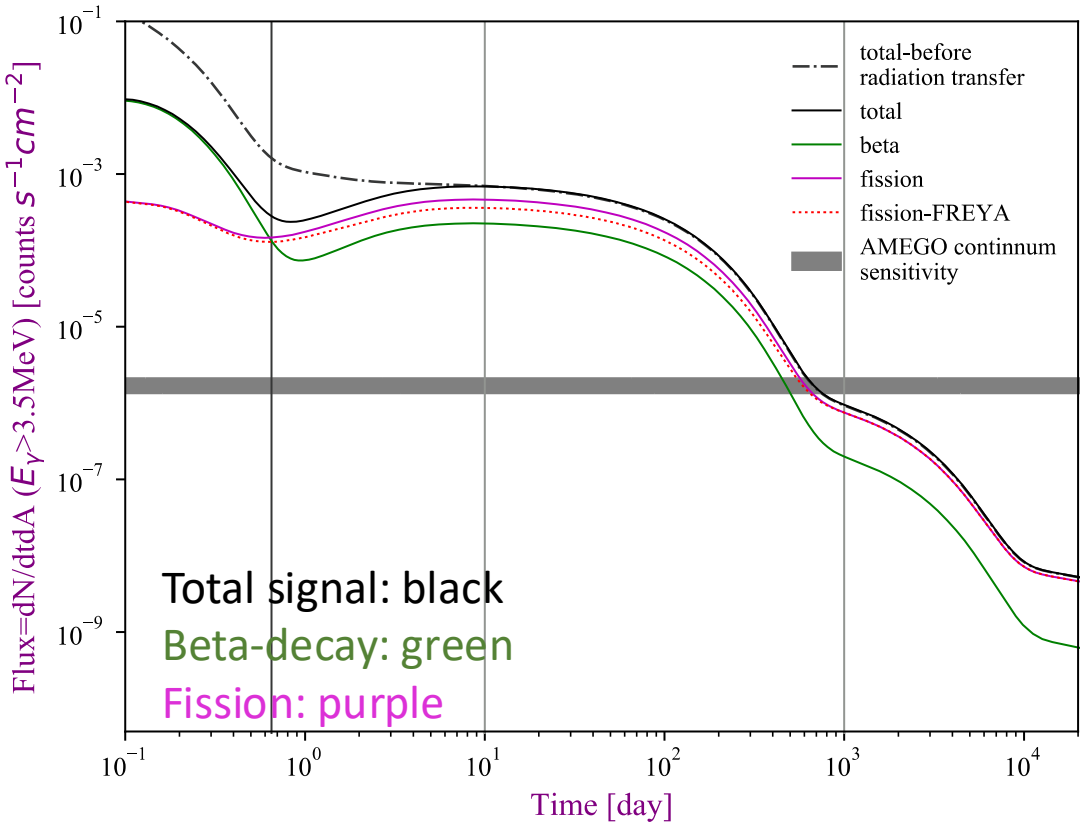


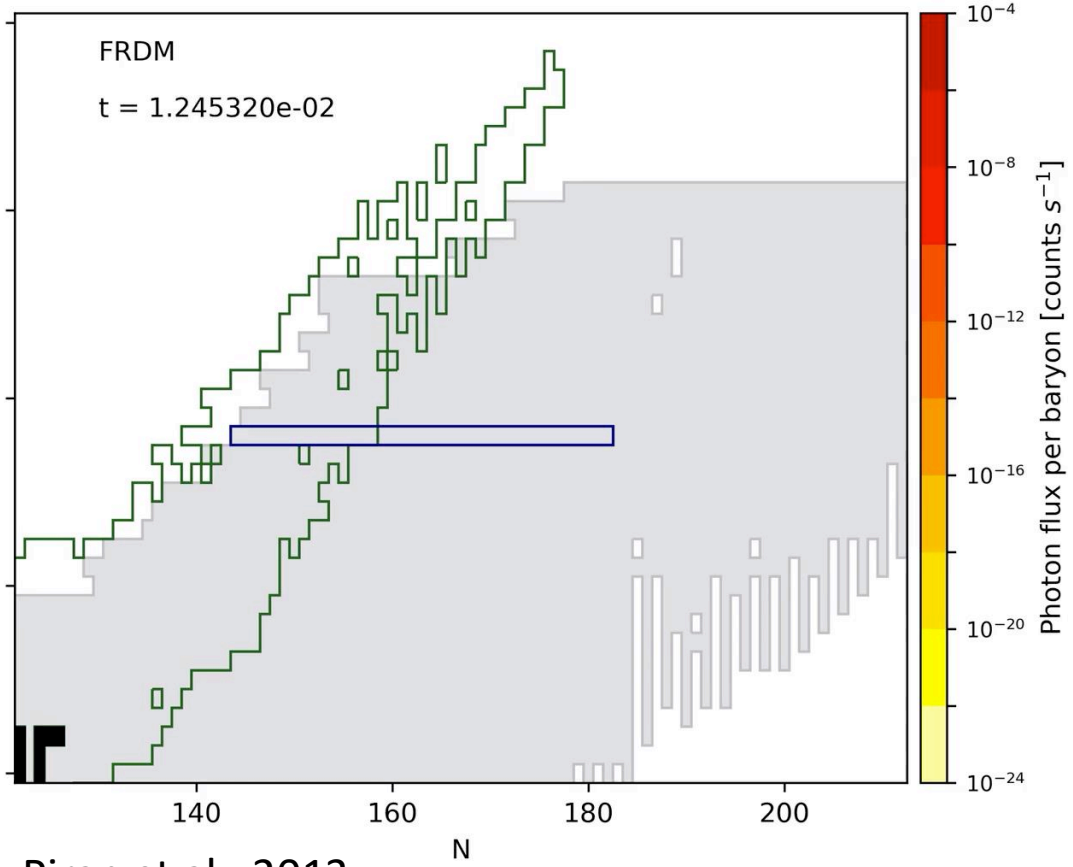
Wang, X., Vassh, N., et al. 2020 , ApJL, 903, L3

MeV light curve and contributions from individual fissioning nuclei



Flux at $E_\gamma > 3.5MeV$

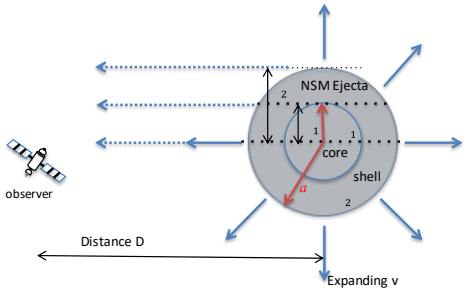




Very neutron rich dynamical ejecta from Rosswog et al., 2013, Piran et al., 2013.
Nuclear data based on FRDM and FRLDM nuclear models

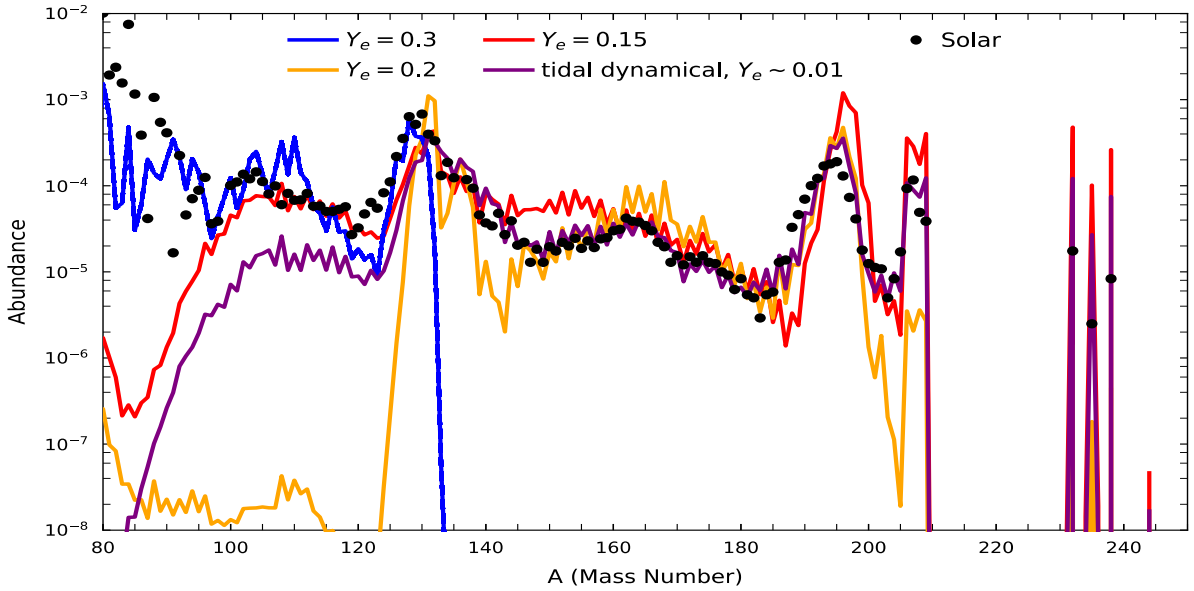
Wang, X., Vassh, N., et al. 2020 , ApJL, 903, L3

Variations on neutron-richness (Y_e) and the actinide production

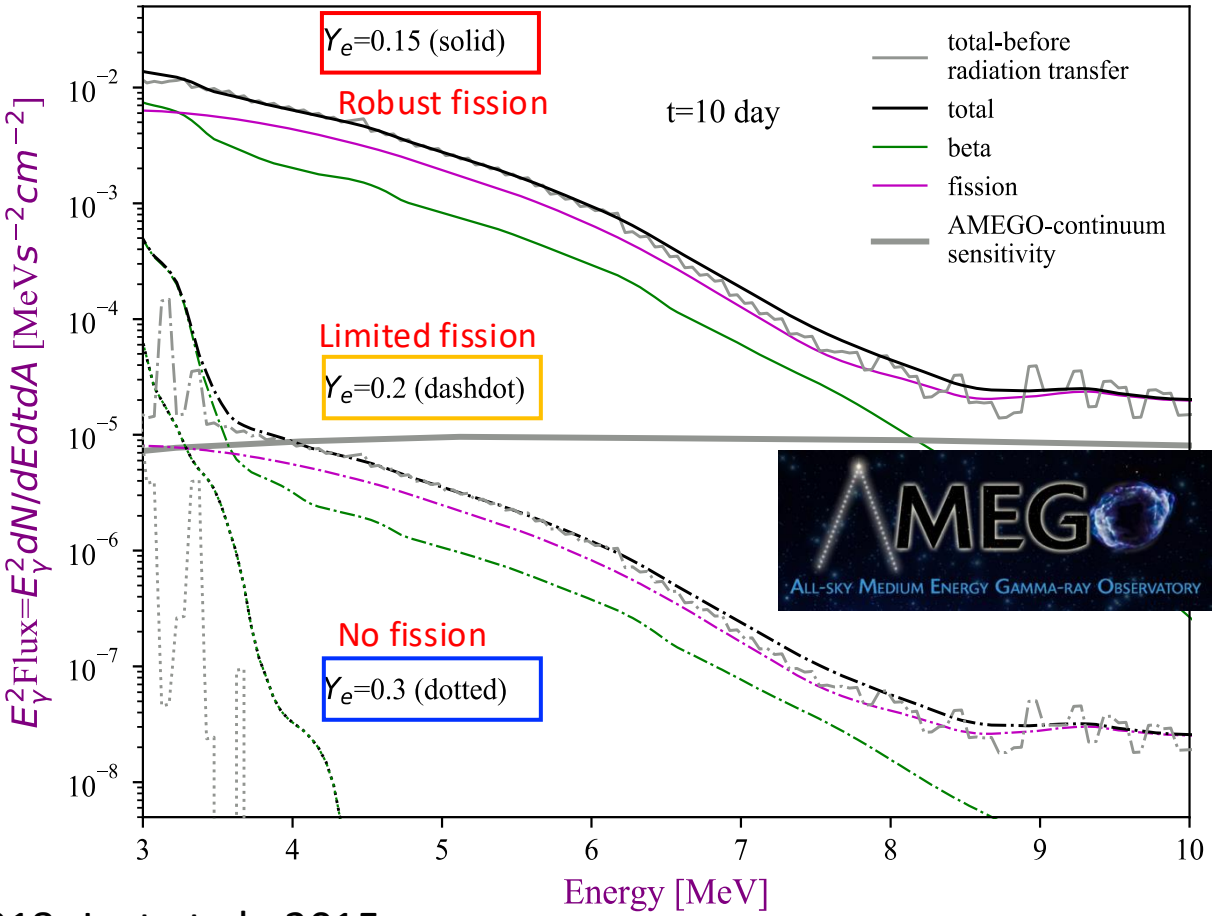


$$Y_e = \frac{n_e}{n_b} = 1 - \frac{n_n}{n_n + n_p}$$

Smaller Y_e: more neutron rich



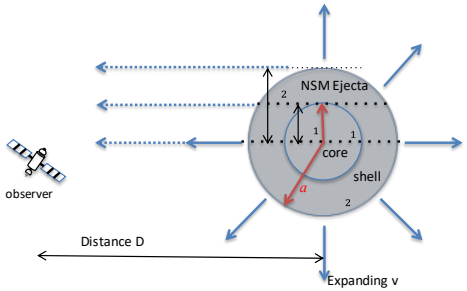
Total signal: black
Beta-decay: green
Fission: purple



Low entropy parameterized outflow found in Radice et al., 2018, Just et al., 2015.
Nuclear data based on FRDM and FRLDM nuclear models

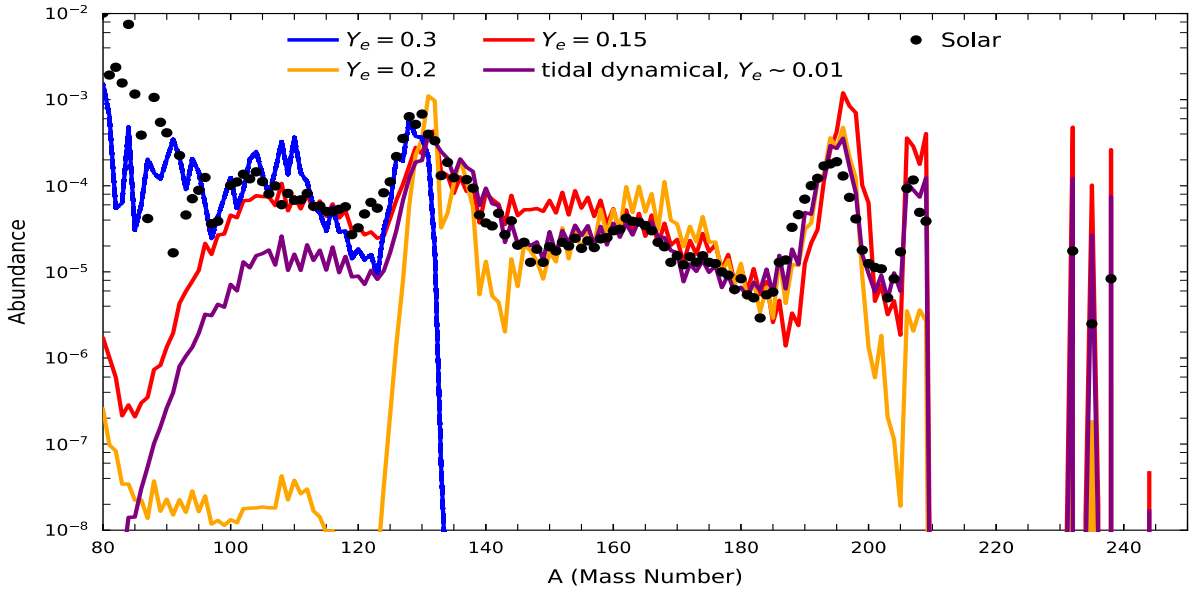
Wang, X., Vassh, N., et al. 2020 , ApJL, 903, L3

Variations on neutron-richness (Y_e) and the actinide production



$$Y_e = \frac{n_e}{n_b} = 1 - \frac{n_n}{n_n + n_p} \sim 0.015$$

Smaller Y_e: more neutron rich

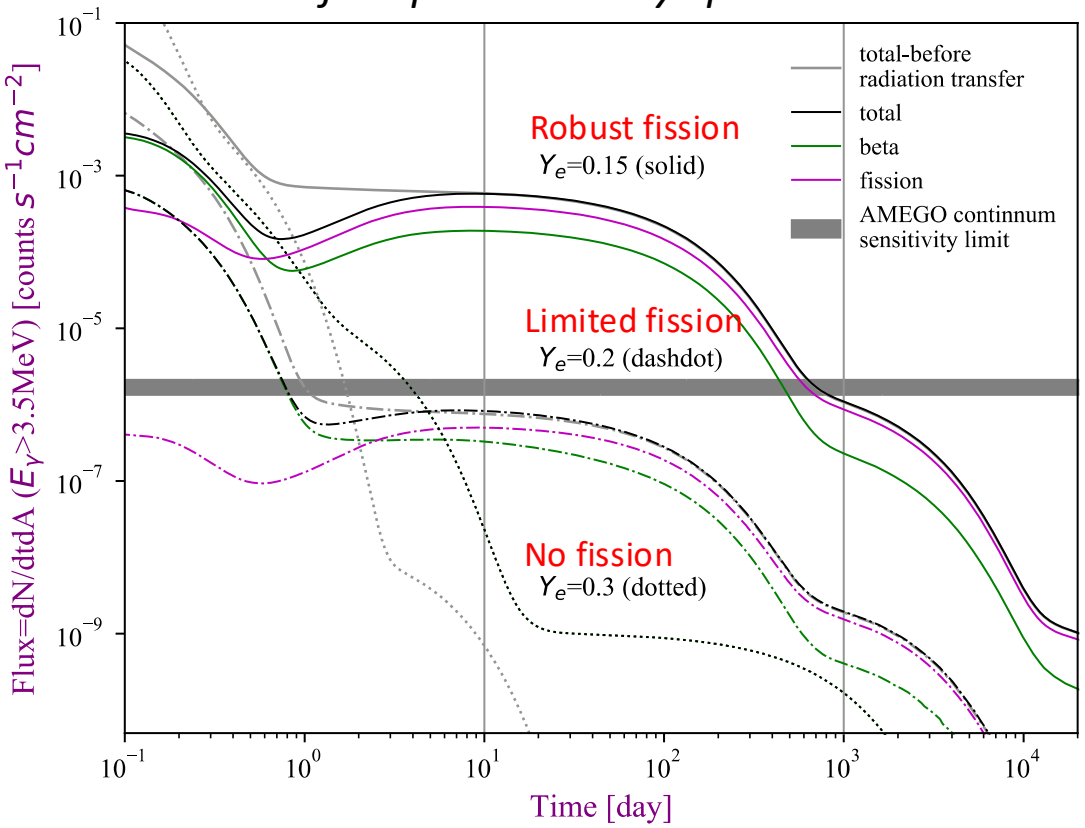


Total signal: black

Beta-decay: green

Fission: purple

Visible for up to 1000 days post-event

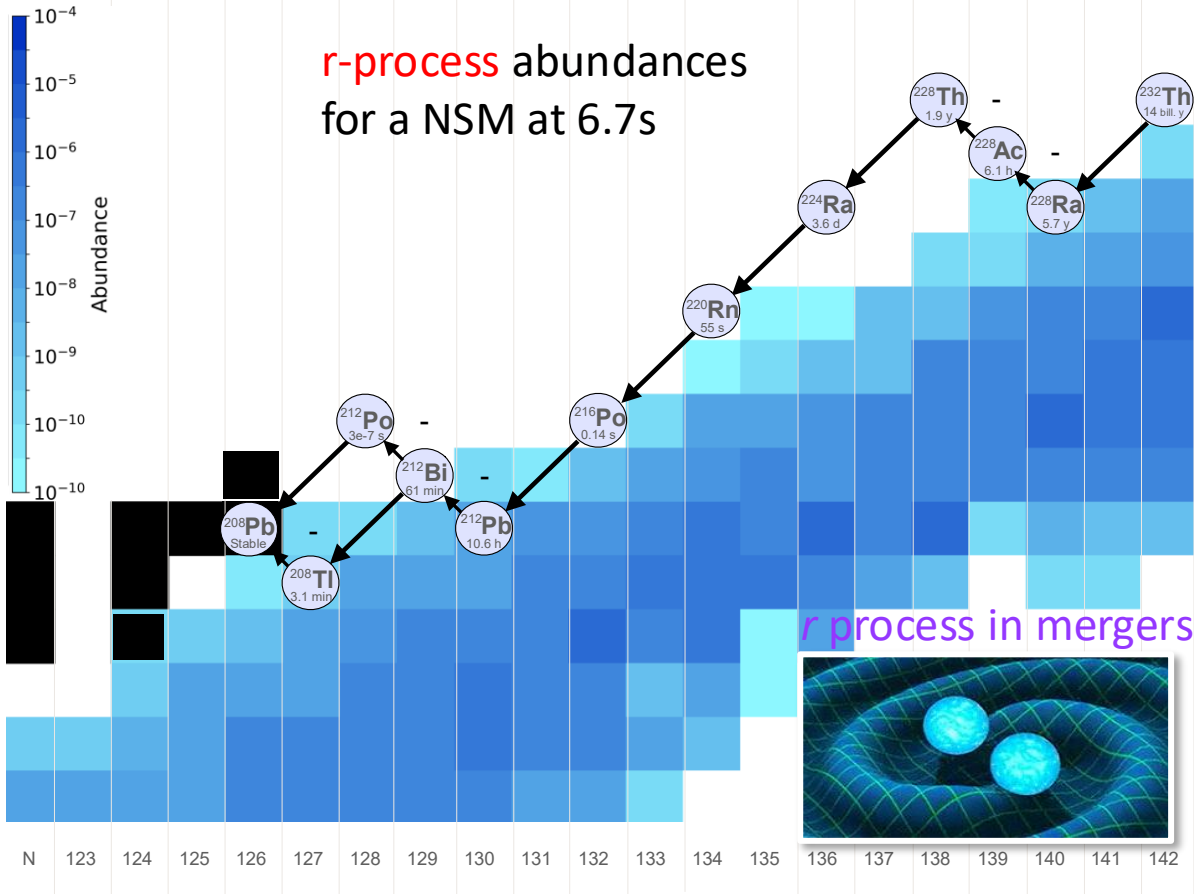


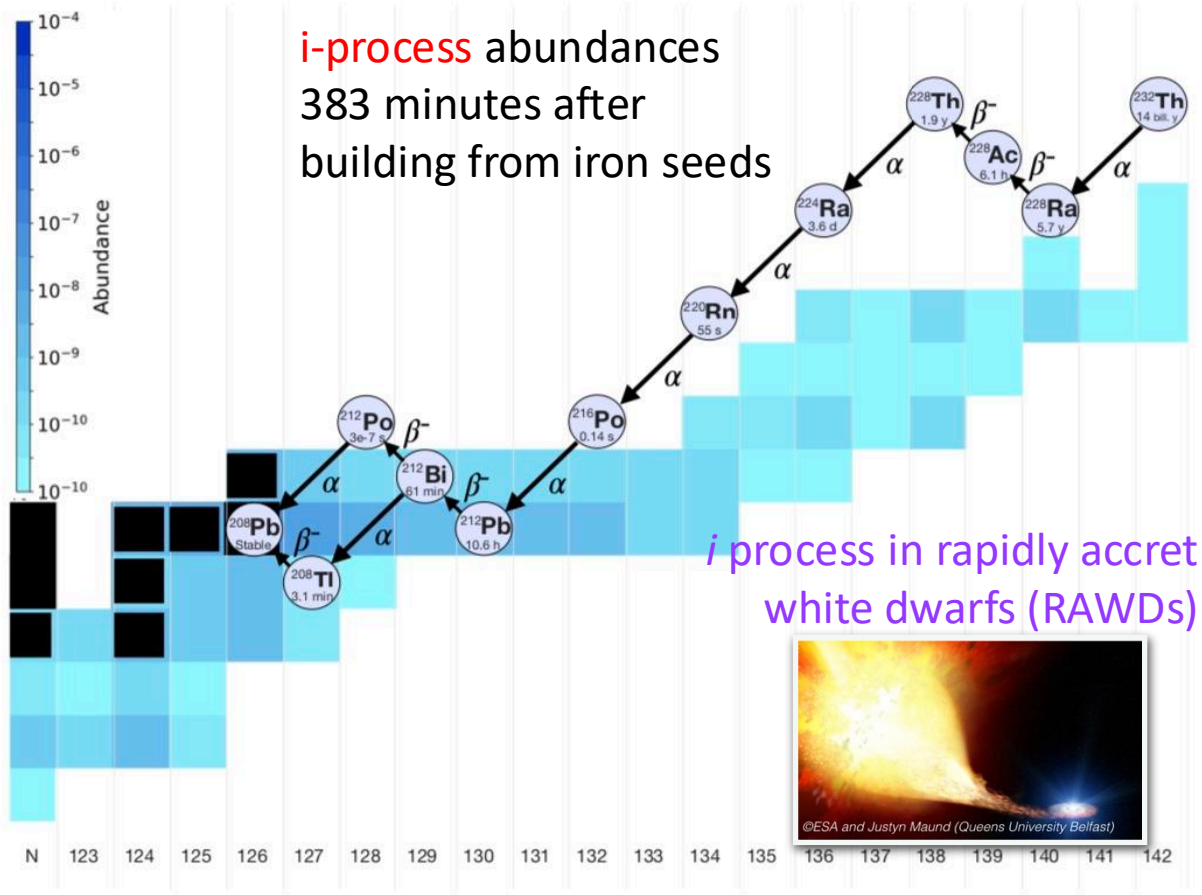
Low entropy parameterized outflow found in Radice et al., 2018, Just et al., 2015.

Nuclear data based on FRDM and FRLDM nuclear models

Wang, X., Vassh, N., et al. 2020 , ApJL, 903, L3

Thallium-208: A Beacon of In Situ Neutron Capture Nucleosynthesis



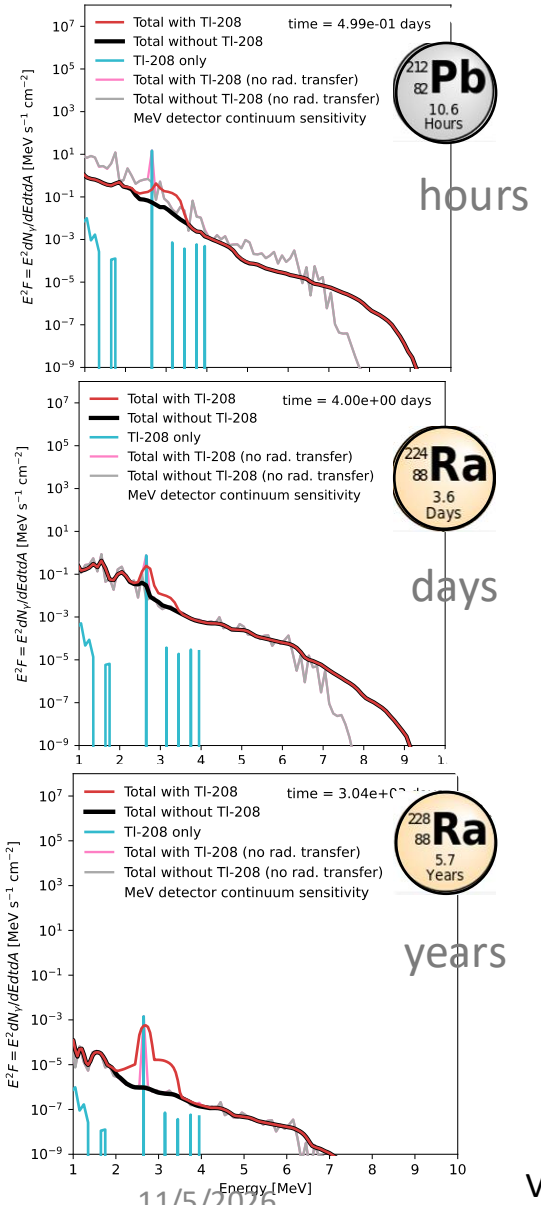


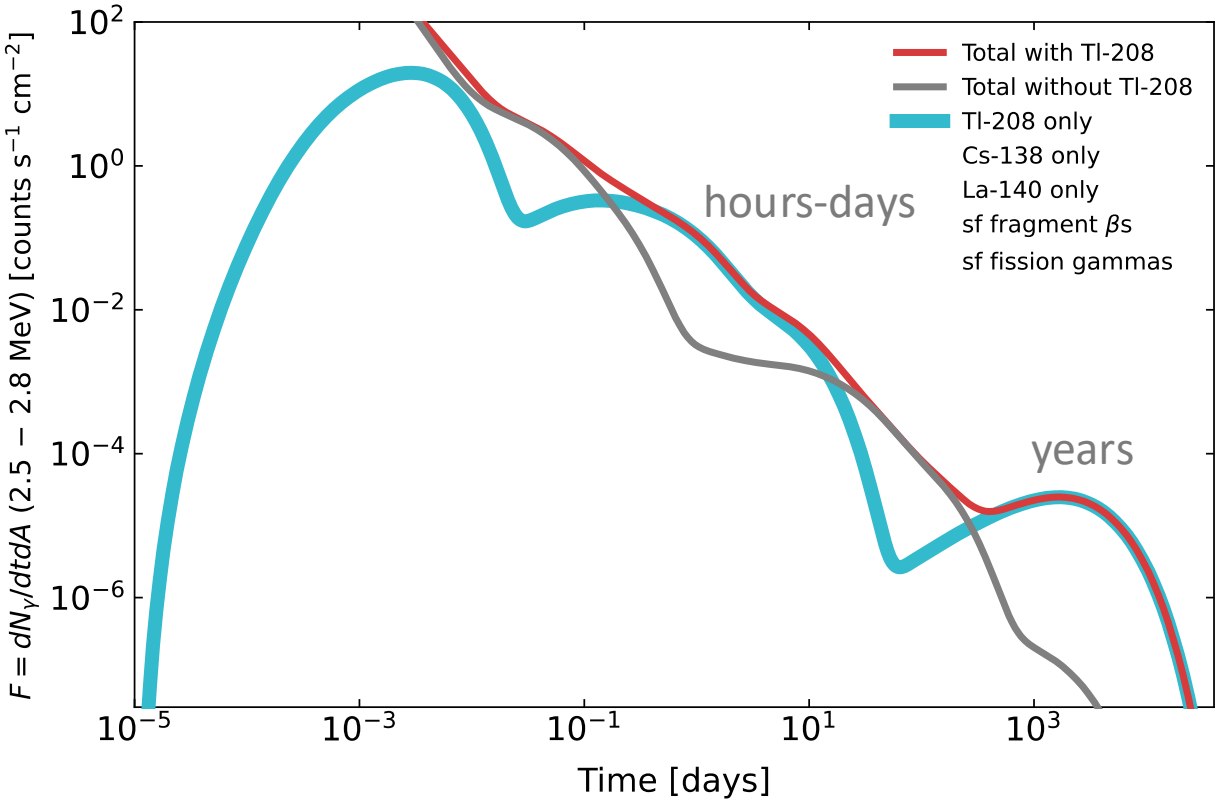
neutron capture processes can populate species along the well-known Th-232 decay chain → yielding Tl-208;

Detection of Tl-208 represents the only identified prospect for a direct signal of lead production (implying 3rd r-process peak synthesis like gold) in a real-time event.

Vassh, N., **Wang, X.**, et al., 2024, PRL, 132, 052701

2.6 MeV Tl-208 lines emitted from neutron star mergers





- the 2.6 MeV Tl-208 line explicitly show itself in the spectrum at the timescales: ~12hours - ~10days (after Tl is populated by Pb-212 and Ra-224 decays); 1-20 years (Ra-228 decays);
- Next generation MeV gamma-ray detectors will be able to detect the Tl-208 lines from NSM in Milky Way or nearby galaxies at these timescales.

Very neutron rich dynamical ejecta from Rosswog et al., 2013, Piran et al., 2013.
Nuclear data based on FRDM and FRLDM nuclear models

Vassh, N., **Wang, X.**, et al., 2024, PRL, 132, 052701

MeV lines from weak … topes in NSMs

NSM simulation: the 1.2 - 1.4 $M_\odot$ NSM results from D. Radice et al. (2018) (assuming M0 neutrino treatment); d-10kpc; M_{ej}=0.01 $M_\odot$

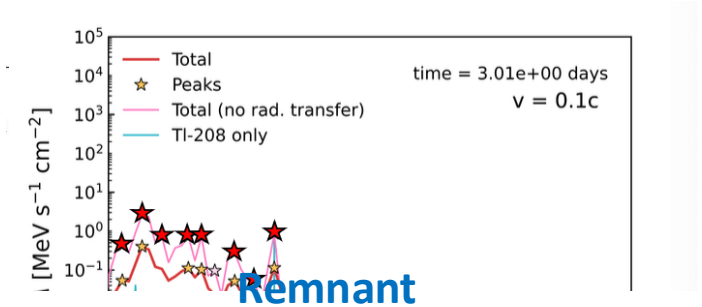
Nuclear variations:

- Nuclear mass models: FRDM2012, HFB27, TF
- β-decay treatments: Moller et al. (top) and Marketin et al. (bottom)

Isotopes/lines search criteria: dominate the total flux (≥50%) in the line emission bin ±0.1 MeV with flux above a detectability threshold of 10^{-7} counts s^{-1} cm^{-2} for **explosion** epoch (t < 10yrs); 10^{-10} counts s^{-1} cm^{-2} for **remnant** epoch (t > 10yrs);

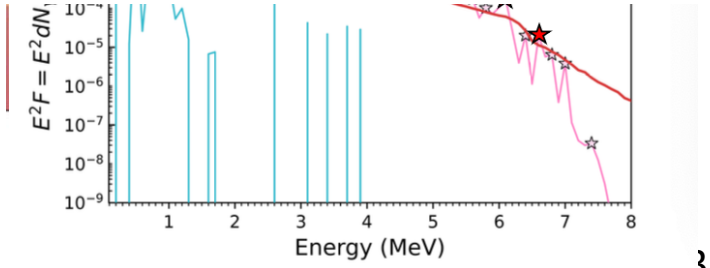
Isotope	Time (days)	E (keV)	Möller β decay	Marketin β decay
Fe-59	8.22e+01 – 1.89e+02	1099	T	T
	6.26e+01 – 2.48e+02	1292	T	T
Ga-72	2.63 – 5.26	1862		H
	8.53e-01 – 1.23e+01	2202	*	*
	7.97e-01 – 1.41e+01	2508	HT	*
	1.56 – 1.48e+01	2844	*FT*	*FHT*
	1.75 – 9.88	**3325**, 3339	*T*	*T*
	1.33 – 6.86	3679		*T*
Rb-88	3.41e-01 – 1.01	3218		*T*
	3.87e-01 – 1.42	4036	T	T
	2.00e-02 – 1.97	4742	*FT*	*FH*T
Nb-95	9.85e+01 – 2.77e+02	766	T	
Ru-103	7.67e+01 – 1.54e+02	497	T	T
Rh-106	2.85e+02 – 1.06e+03	2366	*T*	*T*
Ag-112	8.28e-01 – 2.98	2829	*FT*	*T*
In-128	2.64e-01 – 1.42	4298		T
Sn-125	1.89e+01 – 4.31e+01	**1067**, 1088, 1089		FT
Sb-125	5.03e+02 – 9.62e+02	176		T
	2.48e+02 – 3.89e+03	**428**, 463	FT	*
	3.85e+02 – 8.44e+03	**601**, 636	FT	*
Sb-128	2.67e-01 – 1.53	**743**, 754	FH	*
Sb-134	4.00e-03 – 9.53	6687	*H*	*H*
	5.00e-03 – 5.99	6820	*H*	*H*
I-131	6.59 – 5.43e+01	364	*	FT
I-132	2.56 – 1.95e+01	630, **668**	*	FT
	1.96 – 1.86e+01	773	HT	*T*
	3.29 – 1.27e+01	955	T	T
	2.02 – 2.15e+01	1372, **1399**	*	FT
	1.46 – 1.39e+01	2002	FT	T
I-136	1.00e-03 – 2.12e+02	6104	FH	F*H*
La-140	2.3 – 1.42e+02	1596	*	*
	1.23e+01 – 1.03e+02	2521	*	*
	1.99e+01 – 3.84e+01	2899.6	*T*	*T*
	1.06e+01 – 3.84e+01	3119	T	*T*
Pr-144	2.08e+02 – 1.65e+03	2186	T	H
Eu-156	2.05e+01 – 5.45e+01	**1231**, 1242, 1277		*
	1.41e+01 – 1.27e+02	1938, **1966**	*T*	HT
	1.02e+01 – 1.35e+02	2027, **2098**	*	*
	1.59e+01 – 1.35e+02	2181, **2187**	HT	*HT*
Ir-194	1.32e+03 – 1.45e+04	939		T
	5.78e+02 – 1.57e+04	**1151**, 1183	FT	*
	3.82e+02 – 1.10e+04	1469		FT
	7.14e+02 – 8.44e+03	1622		*T*
	7.14e+02 – 7.23e+03	1806	F*T*	F*T*
Tl-208	8.84e-01 – 1.80e+01	2615	*	
	1.39e+02 – 1.90e+04	2615	*	*
Ac-228	4.45e+02 – 1.61e+04	**911**, 969	FT	H
	5.04e+02 – 1.39e+04	1588	FT	

Explosion



Remnant

Isotope	Time (years)	E (keV)	Nuclear model variations	
			Möller β decay	Marketin β decay
Co-60	4.44e+05 – 4.82e+06	1173	*	*
	1.56e+05 – 4.21e+06	1332	*	*
Rh-106	9.17e-01 – 1.14e+01	2366		*T*
In-128	3.43e+01 – 1.55e+02	3520	F	
Sb-125	6.80e-01 – 1.06e+01	**428**, 463		FT
	1.05 – 2.31e+01	**601**, 636	FT	*
Sb-126	8.74e+01 – 2.10e+06	415	*	*
	5.42e+01 – 2.26e+06	**666**, 695, 697	*	*
	1.95e+04 – 2.10e+05	1213	F	
Sb-134	1.00e-03 – 8.85e+01	6687	*H*	
	1.00e-03 – 3.31e+01	6820	*H*	
I-136	7.00e-03 – 3.02e+02	6104	H	H
Ir-194	9.9 – 7.22e+01	328	FT	*
	3.62 – 4.98e+01	939		T
	1.58 – 7.55e+01	**1151**, 1183	FT	*
	1.05 – 7.00e+01	1469		FT
	1.96 – 7.65e+01	1622		*T*
	1.96 – 7.99e+01	1806	F*T*	*FT*
	5.02 – 5.93e+01	2044		*FT*
Tl-208	8.81e-01 – 1.12e+02	2615	*	*
Tl-209	1.01e+02 – 6.47e+04	1567	*	*
Pb-214	8.17e+01 – 3.21e+03	352	FT	
Ac-228	1.22 – 4.41e+01	**911**, 969	FT	H
	1.38 – 5.18e+01	1588	FT	



MeV lines from weak and ma

Astroph

9 Ye and

- ➢ Ye b
- ➢ Entr
  (ent

Remnant-weak

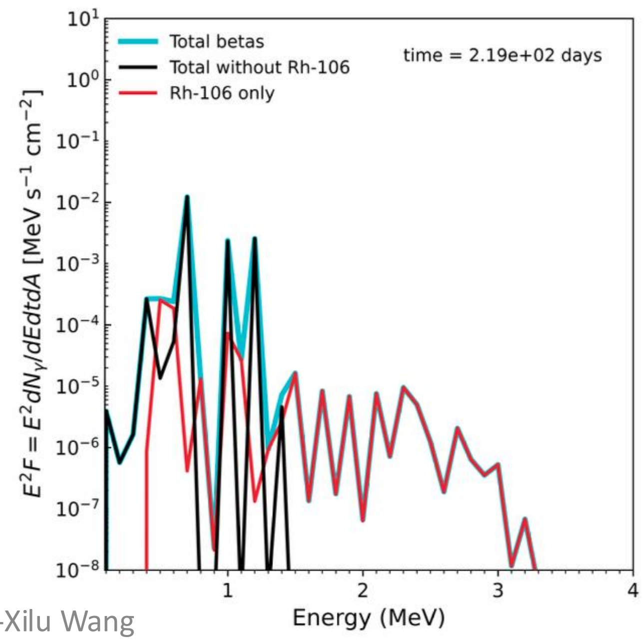
Isotope	Time (years)	E (keV)	Conditions 1	2	3	4	5(r)	6(r)	7	8
K-42	9.76 – 2.89e+02	1525					FH			*
	1.75e+01 – 1.82e+01	1921								F
Co-60	1.43e+01 – 1.40e+07	1173			H	*		*	*	
	8.10 – 1.40e+07	1332			H	*		*	*	
Kr-85	8.47 – 1.51e+02	514		H	H	FH		*	*	
Rh-106	2.34 – 1.63e+01	873			*	*		*FHT*	*	*
	2.07e-01 – 1.90e+01	1050	*	*	*	*	*	*	*	*
	1.20e-01 – 1.90e+01	1562	*	*	*	*	*	*	*	HT
	9.70e-02 – 1.79e+01	**1766**, 1797	*	*	*	*	*FHT*	*	*	*
	1.61e-01 – 1.72e+01	1927, **1988**	*	*	*	*	*	*	*	*
	1.61e-01 – 1.72e+01	2113	*	*	*	*	*	*	*	*
	1.09e-01 – 1.78e+01	2366	*	*	*	*	*	*	*	*
	2.80e-02 – 1.73e+01	2406					F			H
	3.40e-02 – 1.46e+01	2705, **2710**	*	*	*	*	*	T	*	*
	2.40e-02 – 1.24e+01	3037	T		*		*FHT*			*
Sb-125	9.90e-02 – 4.25e+01	176	*	*	*	*	*	*	*	*
	3.19e-01 – 4.51e+01	**428**, 463	*	*	*	*	*		T	*
	6.27e-01 – 3.91e+01	**601**, 636	*	*	*	*	*		FT	*
Sb-126	4.36e+01 – 2.54e+06	415	*	*	*	*	*	*	*	*
	3.77e+01 – 2.92e+06	**666**, 695, 697	*	*	*	*	*	*	*	*
	1.35e+01 – 1.17e+06	1213	*	*	FT		*			*
	1.57e+01 – 3.36e+05	1477	*	FT	F		*			*

id	Y_e, s/…				
1	0.01, 1…				
2	0.01, 3…				
3	0.01, 7…				
4	0.07, 1…				
5	0.07, 32	13	0.19, 10	5	0.29, 75
6	0.07, 75	14	0.19, 32	6	0.32, 10
7	0.13, 10	15	0.19, 75	7	0.32, 32
8	0.13, 32			8	0.32, 75

Mas

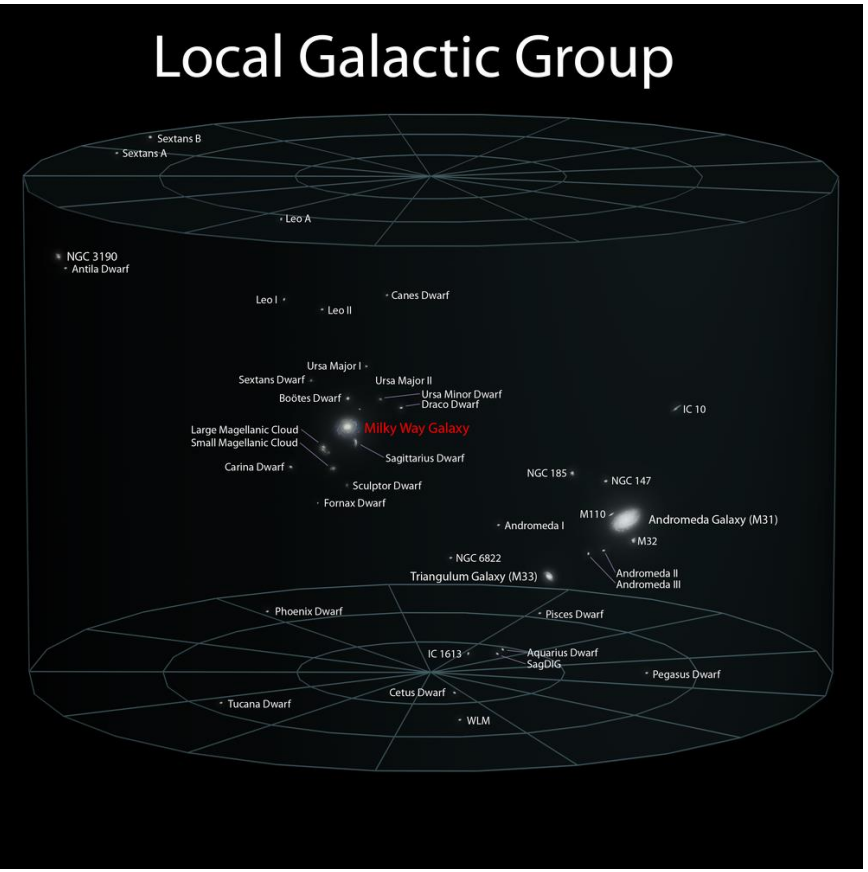
Remnant-main

Isotope	Time (years)	E (keV)	1(r)	2	3	4	5	6	7	8	9	10	11	12	13	14(r)	15
Rh-106	3.37e-01 – 1.40e+01	2366														*FHT*	
	4.70e-01 – 1.39e+01	2406														*H*	
In-128	3.44e+01 – 1.38e+02	3520	*F*	F	F	F	F	F	F	F	F		F	F			F
	8.22e+01 – 8.64e+01	4298	F														
Sb-125	3.37e-01 – 1.40e+01	176														FT	
	4.06e-01 – 2.28e+01	**428**, 463														*	
	8.95e-01 – 3.07e+01	**601**, 636											FH			*	
Sb-126	6.32e+01 – 2.18e+06	415	*	*	*	*	*	*	FT	*	*	HT	*	T	FH	*	FH
	4.06e+01 – 2.56e+06	**666**, 695, 697	*	*	*	*	*	*	*	*	*	*	*	*	*	*	*
	4.66e+01 – 1.72e+06	954, **990**														*FHT*	
	7.25e+01 – 8.86e+05	1213	FT	FT		FT	FT	FT	*	*	*		FH	T	FH	*	
	8.41e+01 – 6.87e+04	1477														FH	
Sb-134	1.00e-03 – 1.98e+02	6687	*H*	H	H	H	H	H	H	H	H			H			
	1.00e-03 – 1.16e+02	6820	*H*	H	H	H	H	H	H	H	H			H			
I-136	1.00e-03 – 5.99e+02	6104	F*H*	FH	FH	FH	FH	FH	FH	FH	FH	H		FH			
Eu-155	2.59 – 3.87e+01	105			T										H	H	
Ta-182	1.55e+03 – 3.74e+06	**1121**, 1189	H	H	H	H	H	H		H		H	H		H		H
	1.48e+03 – 3.47e+06	**1221**, 1231	H	H	H	H	H	H		H		H	H		H		H
Ir-194	5.20e-01 – 8.27e+01	328	FT	FT	F	FT	FT	FT	FT	FT	FT	*	*	FT	*	*	*
	1.42 – 5.78e+01	645													FH		H
	9.55e-01 – 6.47e+01	939													H	*	H
	4.51e-01 – 8.99e+01	**1151**, 1183	FT	FT	FT	FT	FT	FT	FT	FT	FT	*	*	FT	*	*	*
												H	*		*	*	*
															H	*FHT*	H
													H		FH		FH
						FT	FT	FT	FT	FT	FT	*	*	FT	*	*FHT*	*
													FT		*	*FHT*	*
						FT	FT	FT	FT	FT	FT	FT		FT	T		T
						*	*	*	*	*	*	*	*	*	*	*	*
							T						T		T		T
															T		T
						*	*	*	*	*	*	*	*	*	FT		*
							T	T		T	T	FT	T	T	T		FT
						*	*	*	*	*	FT	*	FT	*	FT		*
						FT	FT	FT	FT	FT	FT	FT	FT	FT	T		FT
						FT	FT	FT	FT	FT	FT	FT		FT			T
								H	FH		H			FH			
						T			T								
	1.22e+02 – 3.68e+02	**834**, 839		T		T	T	T	T	T		T		T			



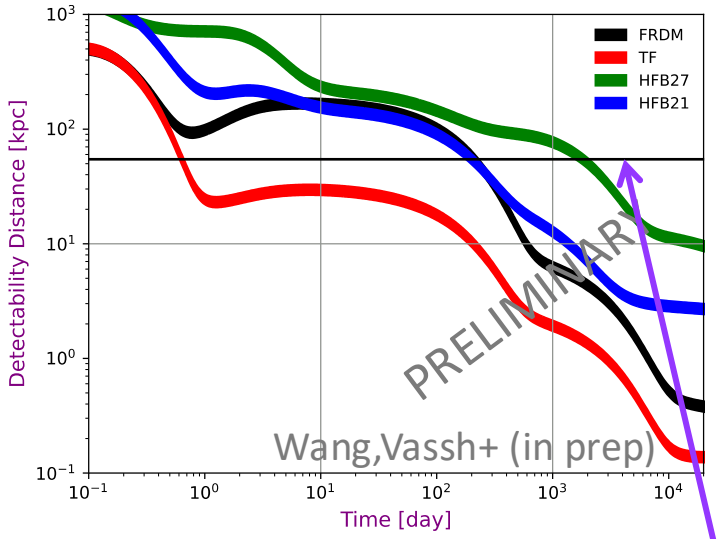
Rh-106: a unique opportunity to distinguish between main and weak r-process emission

From how far could we see signals given projected detector sensitivity?

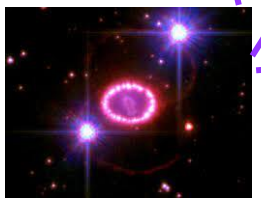


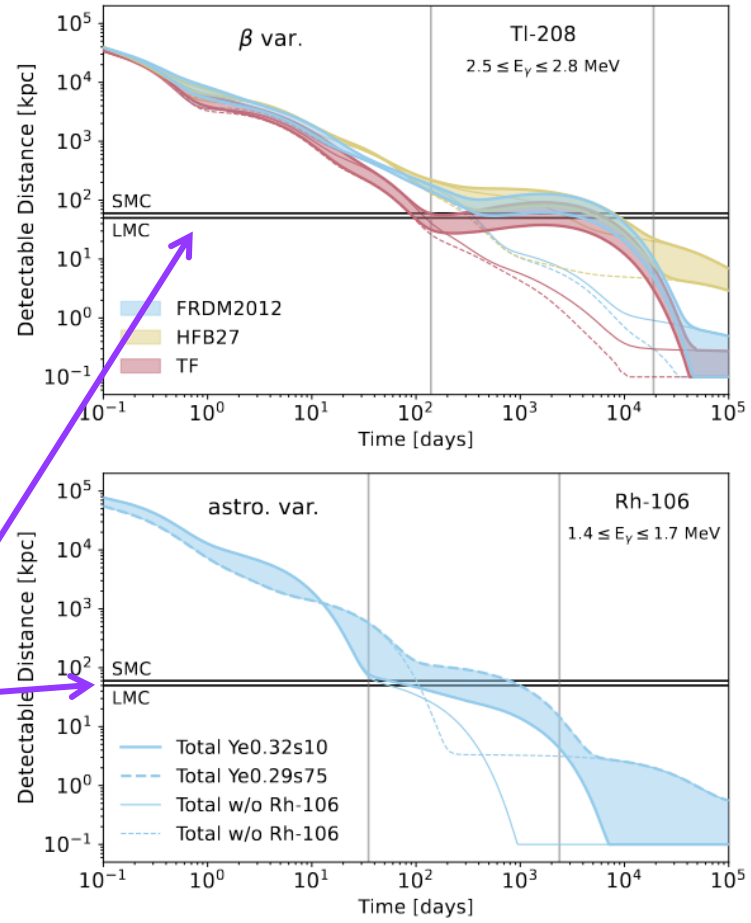
Detectability of **fission gammas** (>3.5 MeV) and **Tl-208 2.6 MeV gamma line & Rh-106 1.56 MeV gamma line** with the next general MeV telescope:

predicted detectability distance depends on nuclear model assumptions and astrophysical conditions of the outflow



SN1987A

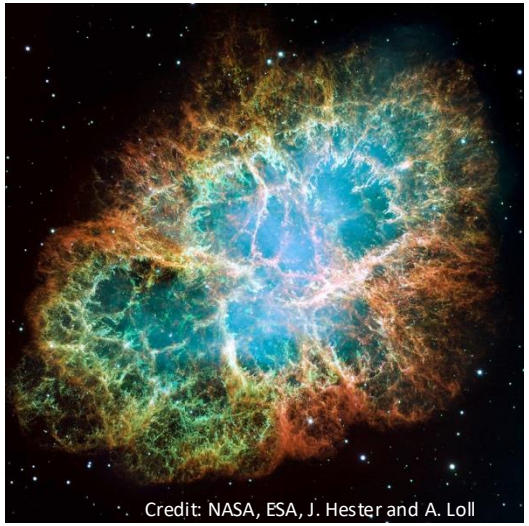




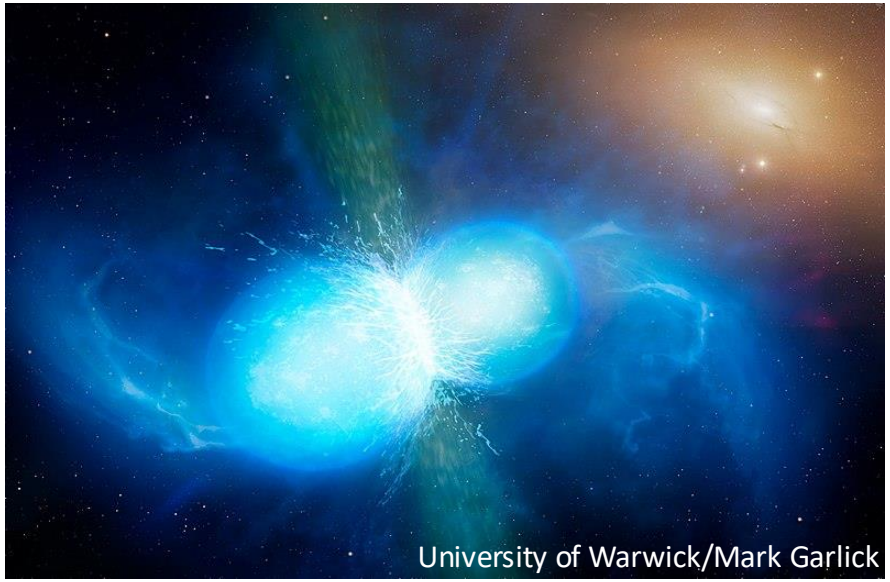
Larivière, M., **et al.**, arXiv:2605.17213

r-process sites: a mystery

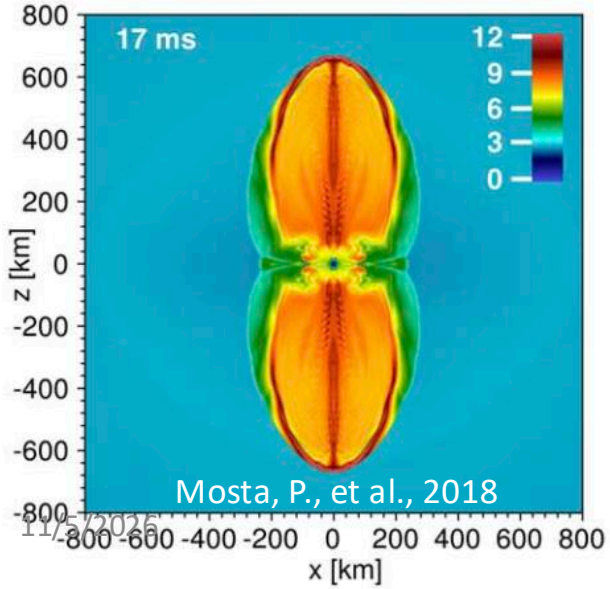
Core collapse Supernovae?
(e.g., Meyer+1992, Roberts+2012)



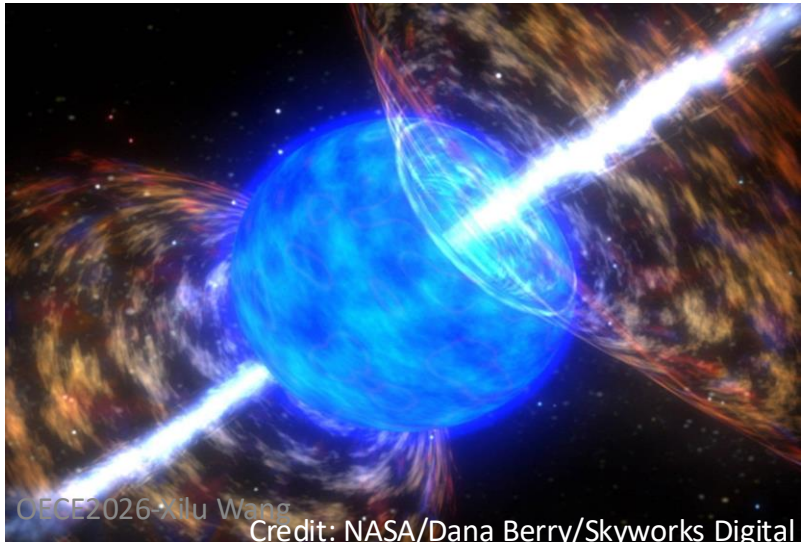
Neutron star + neutron star/black hole mergers
(e,g, Nedora+2020, Foucart+2020, George+2020, etc.)



Magneto-rotational supernovae
(e.g., Reichart+2020, Nishimura+2017, Mosta+2018)



Collapsars
(e.g., Siegel+2019, Miller+2019)



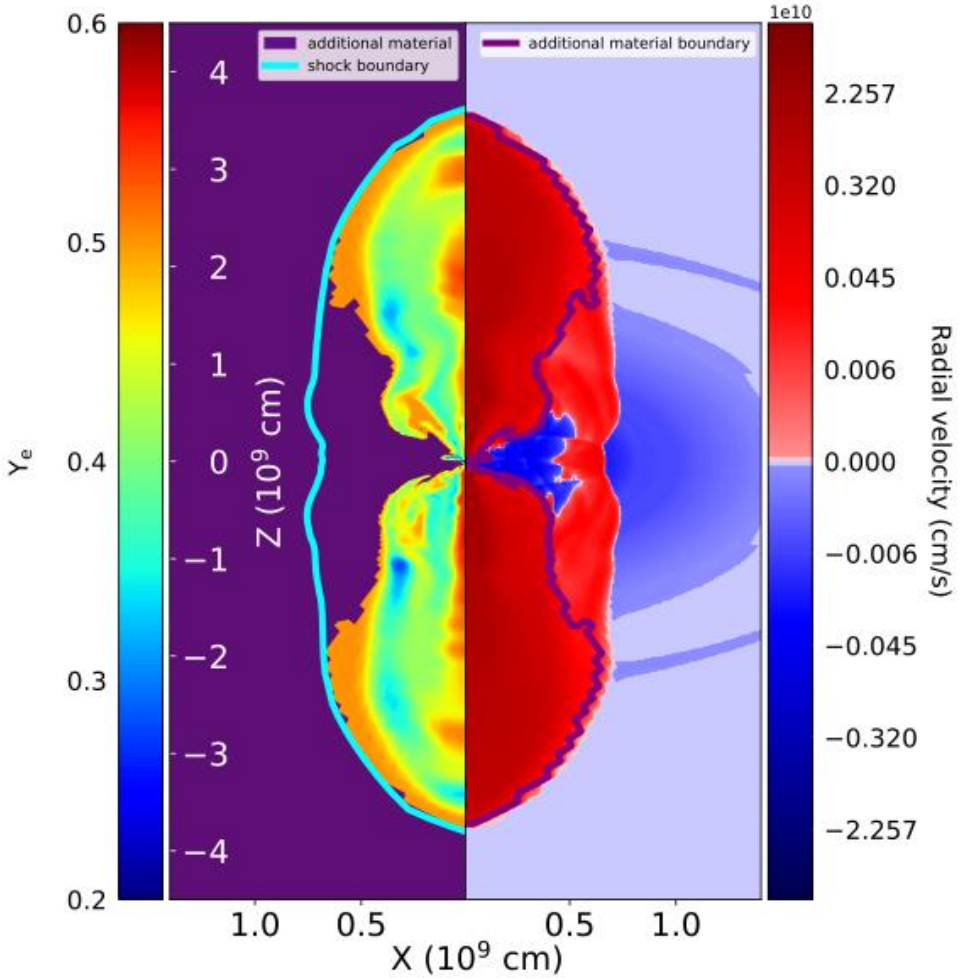
Magnetar giant flare
(Patel+2025)

exotic supernovae
(e.g., Fischer+2020)

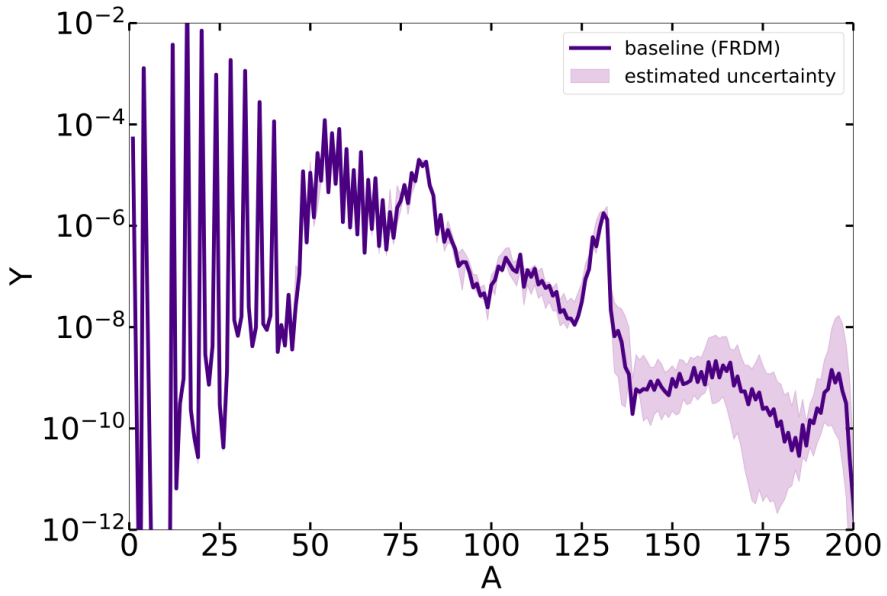
primordial black hole + neutron star (e.g., Fuller+2017)

etc.

MeV gamma-ray from rare supernovae with r-process



Snapshot of the MR-SN model 35OC-RS from Reichert et al. (2021) at the end of the simulation time (1.306 s).



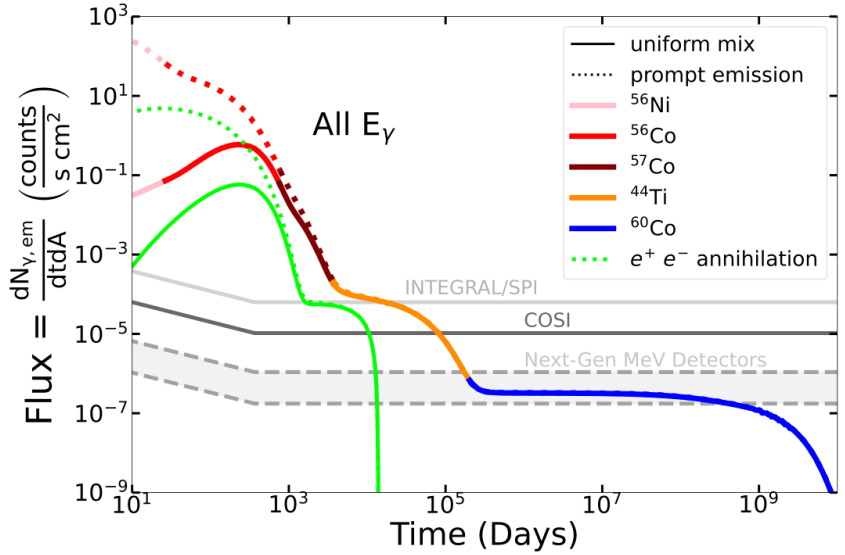
Abundance patterns from the MR-SN model 35OC-RS tracers from Reichert et al. (2021)

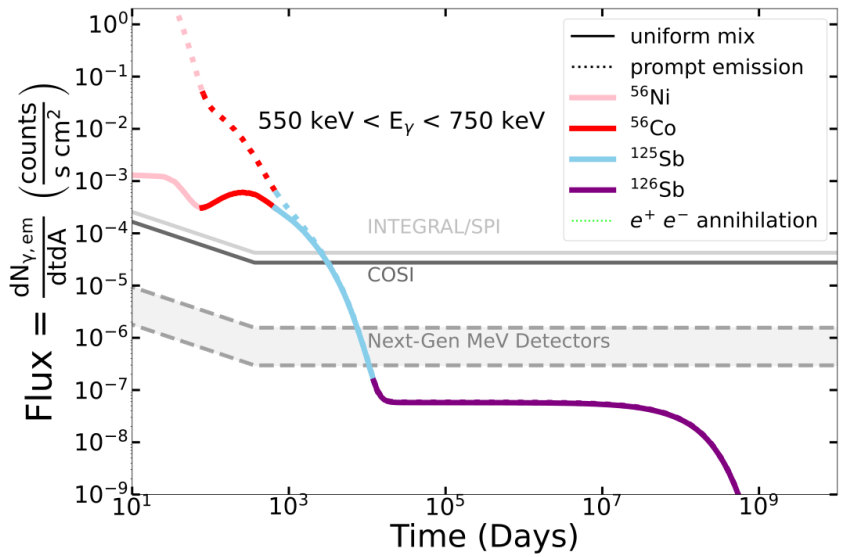


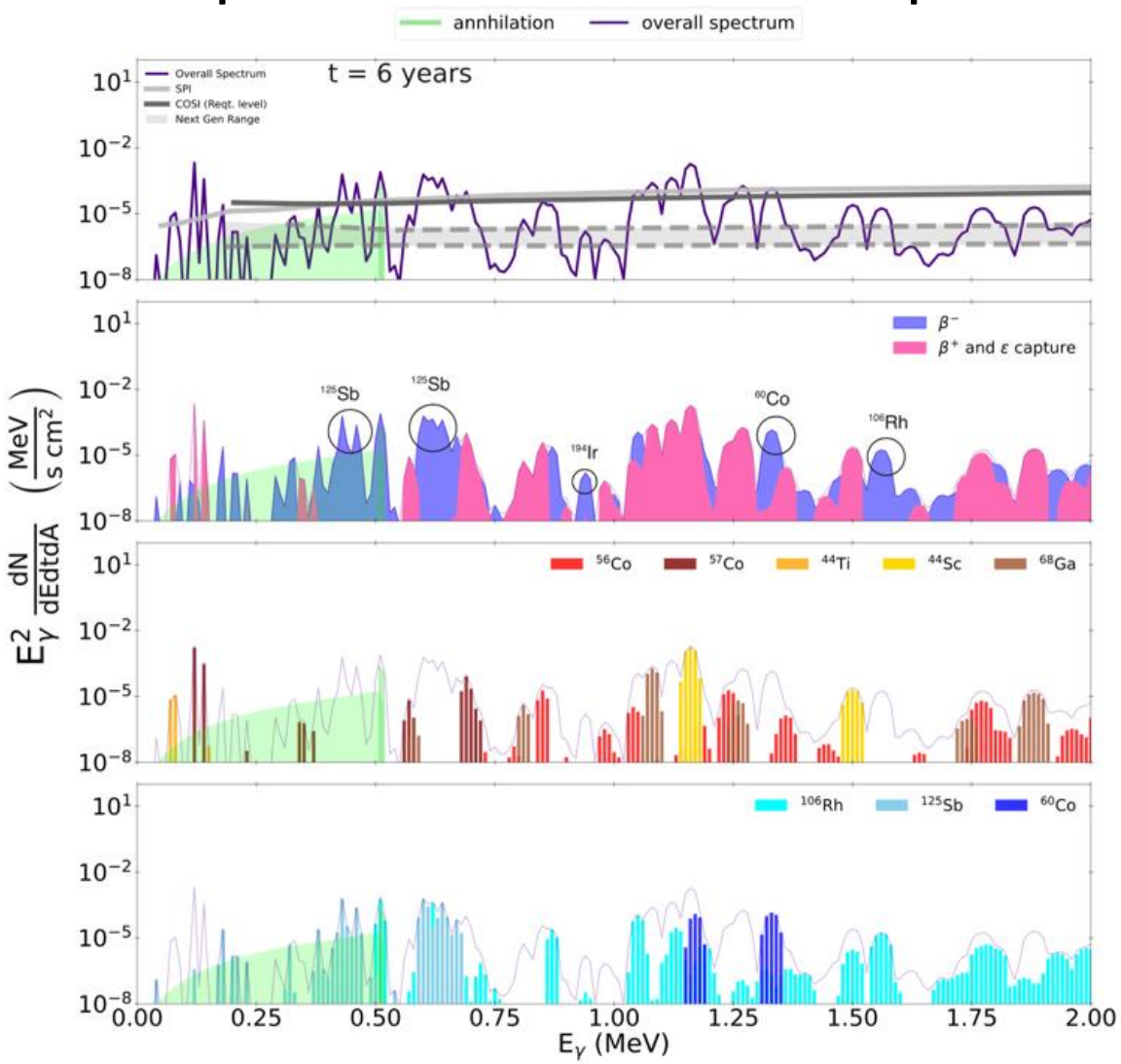
Zhenghai Liu
North Carolino State University

Liu, Z., **et al**., 2025, ApJ, 995, 1, 34

MeV gamma-ray from rare supernovae with r-process



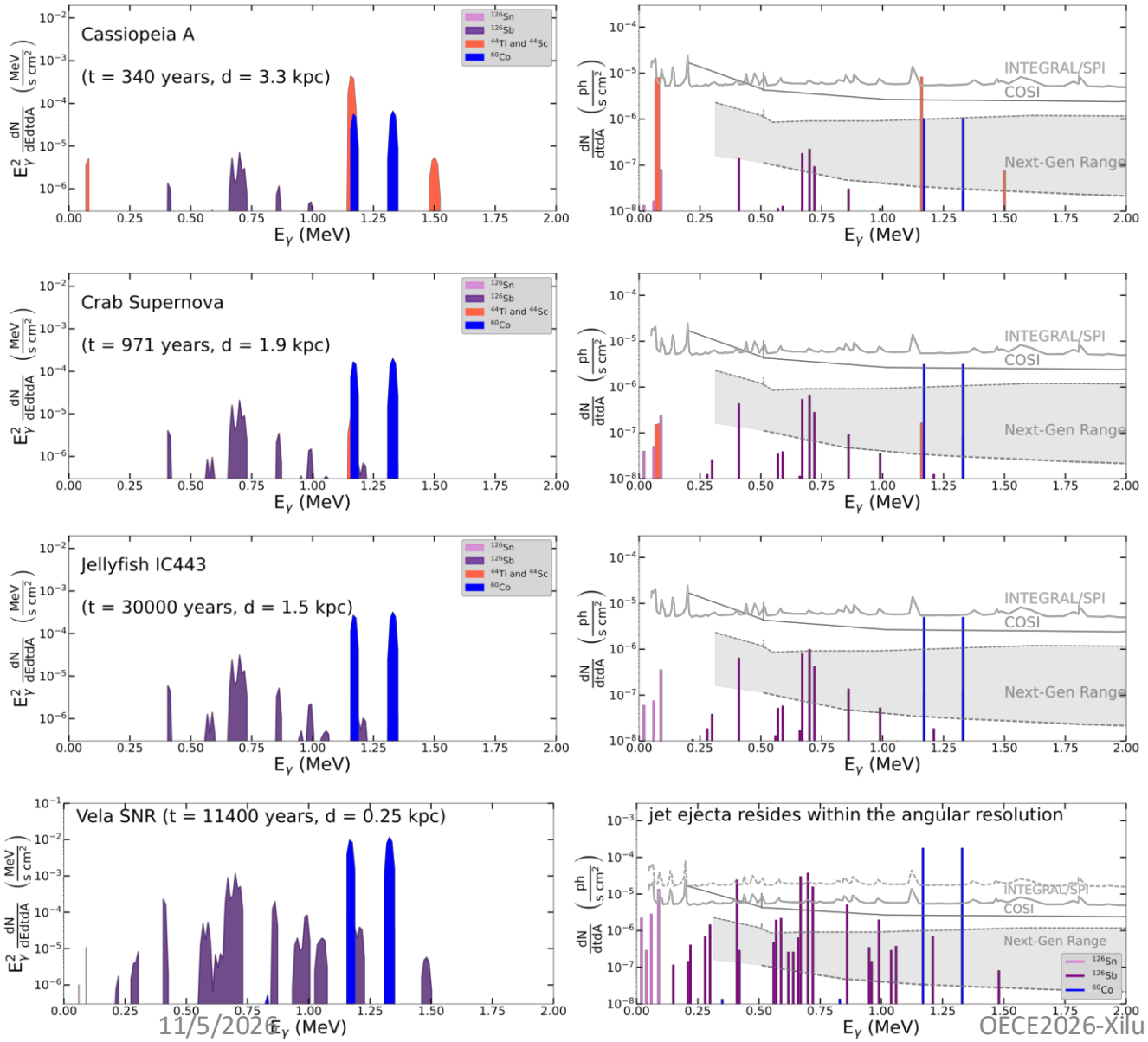


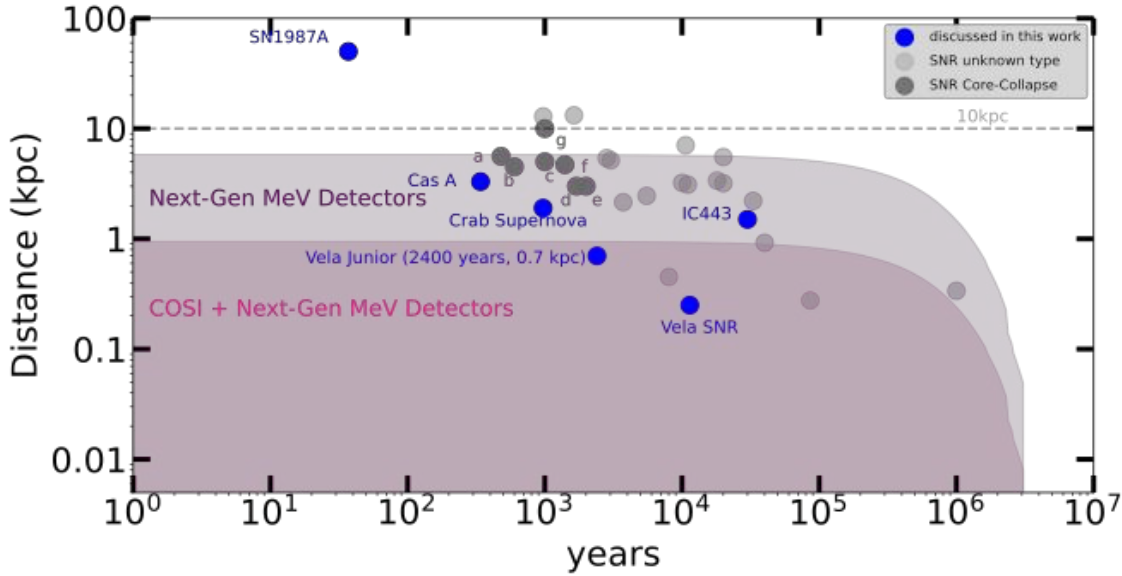


- MeV gamma-ray spectra: prominent *r*-process isotopes features like ^{106}Rh and ^{125}Sb in addition to Fe group isotopes

Liu, Z., **et al**., 2025, ApJ, 995, 1, 34

MeV gamma-ray from rare supernovae with r-process



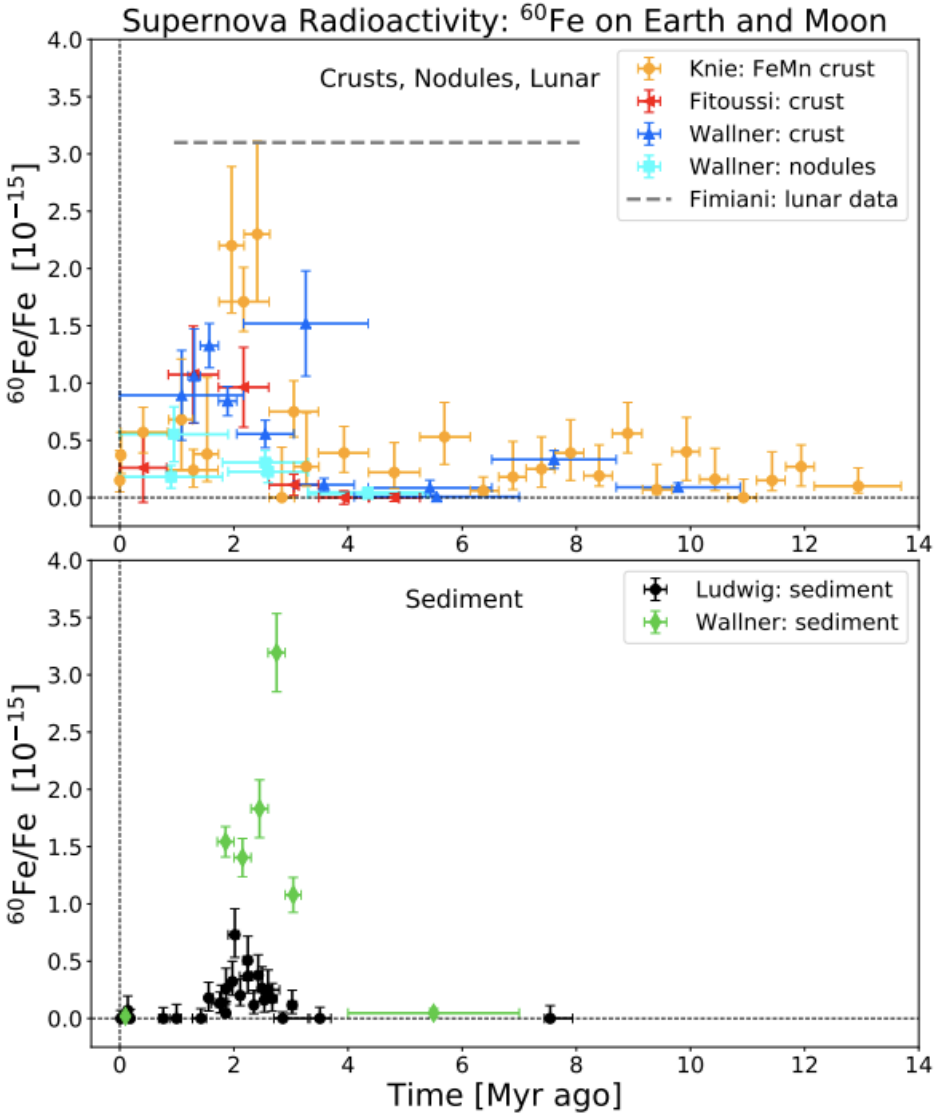


Observability of ^{126}Sb 666 keV line with COSI and next-generation MeV telescopes if a supernova remnant originated from a rare magneto-rotational-SN with r-process occurs.

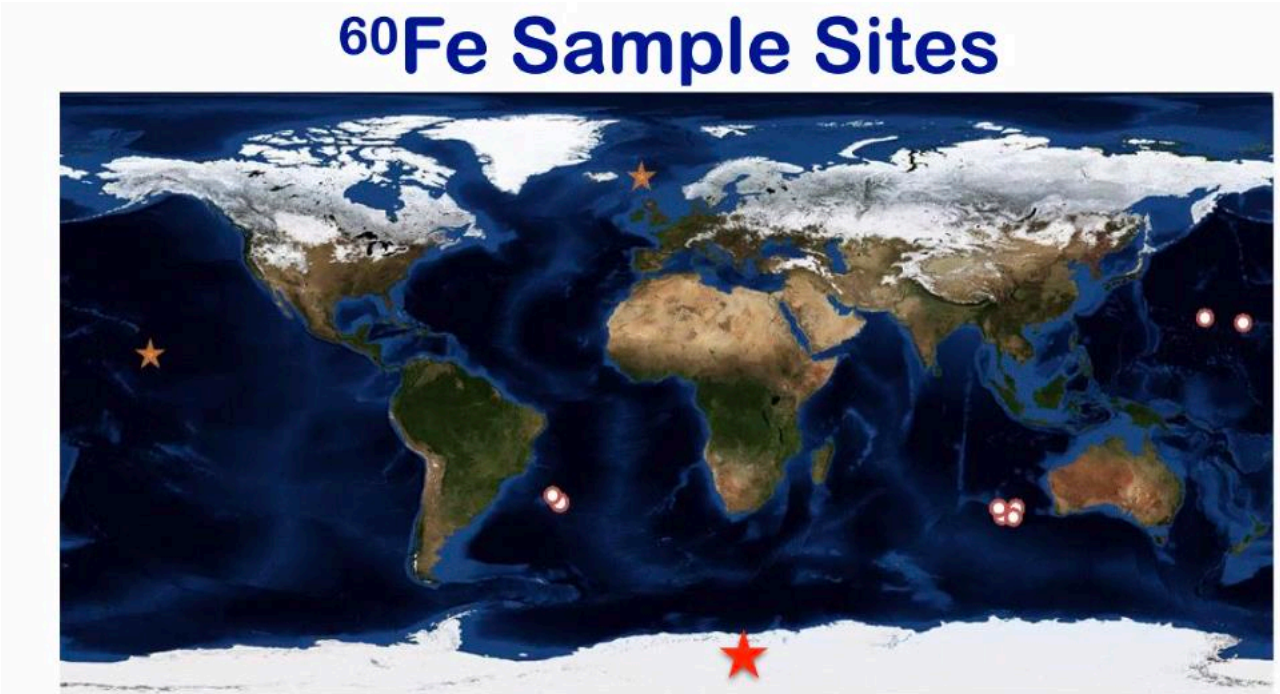
Liu, Z., **et al**., 2025, ApJ, 995, 1, 34

Another interesting astrophysical observables to be explored……

Live radioisotope measurements on the Earth and moon --- ^{60}Fe

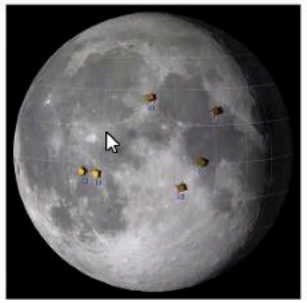


Fields, B., et al. 2019, BAAS, 51,410



$t_{mean,^{60}_{26}Fe} = 3.78\ Myr$

Near-earth event:
within~100pc;
occur ~ 3Myr ago



Credit: Brian Fields

Geological Signatures

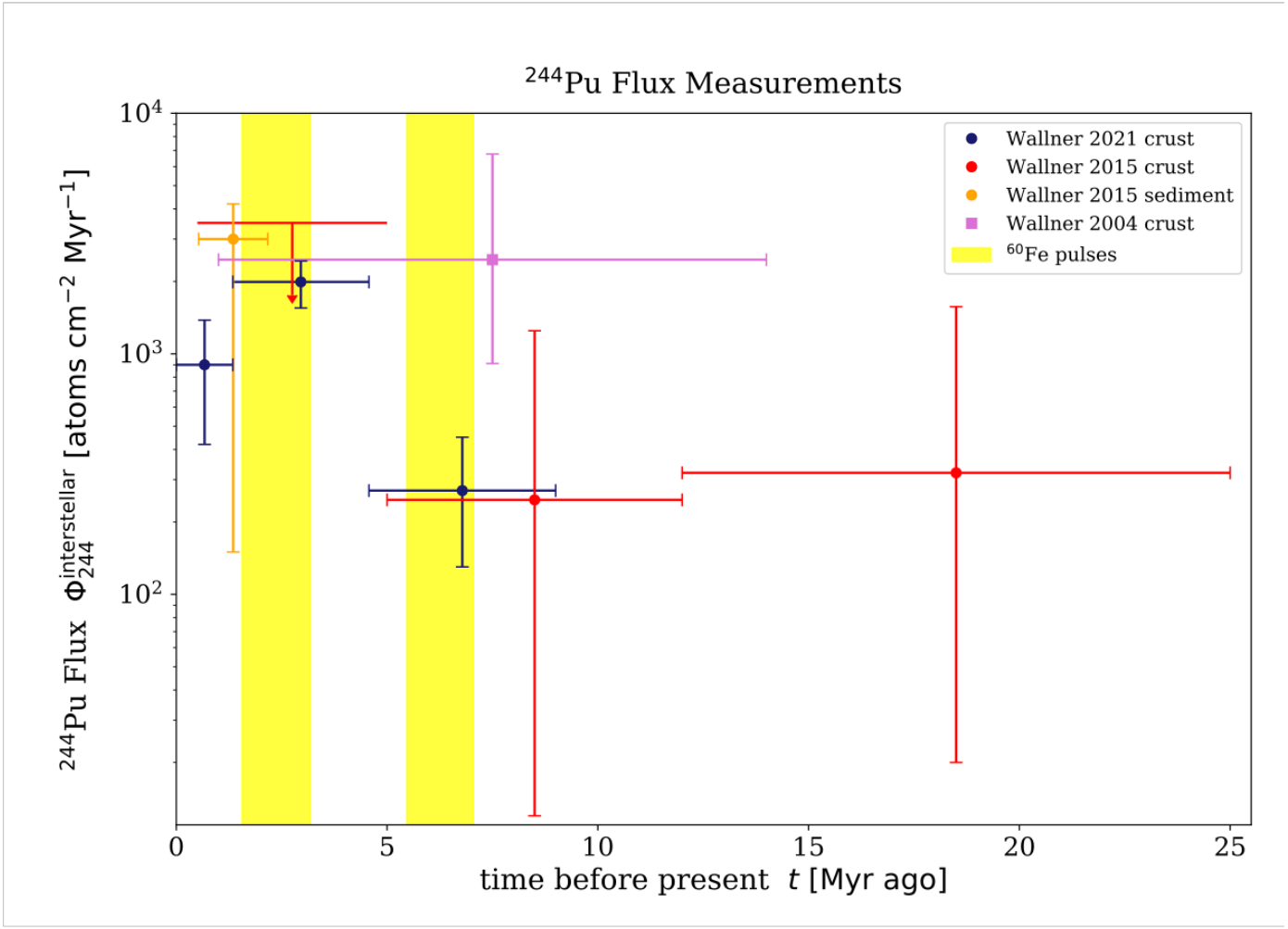


Ferromamanganese (FeMn) Crust

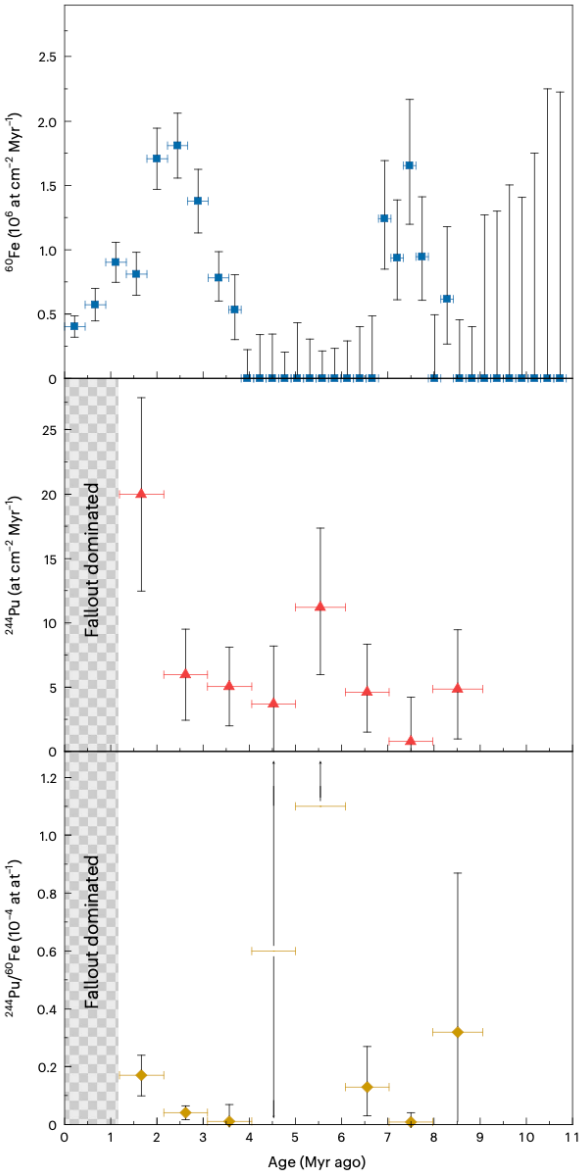
AMS:
Accelerator Mass Spectrometry

Credit: Brian Fields

Live radioisotope measurements on the Earth and moon --- ^{244}Pu



Wang, X., et al., 2021, ApJ 923, 219



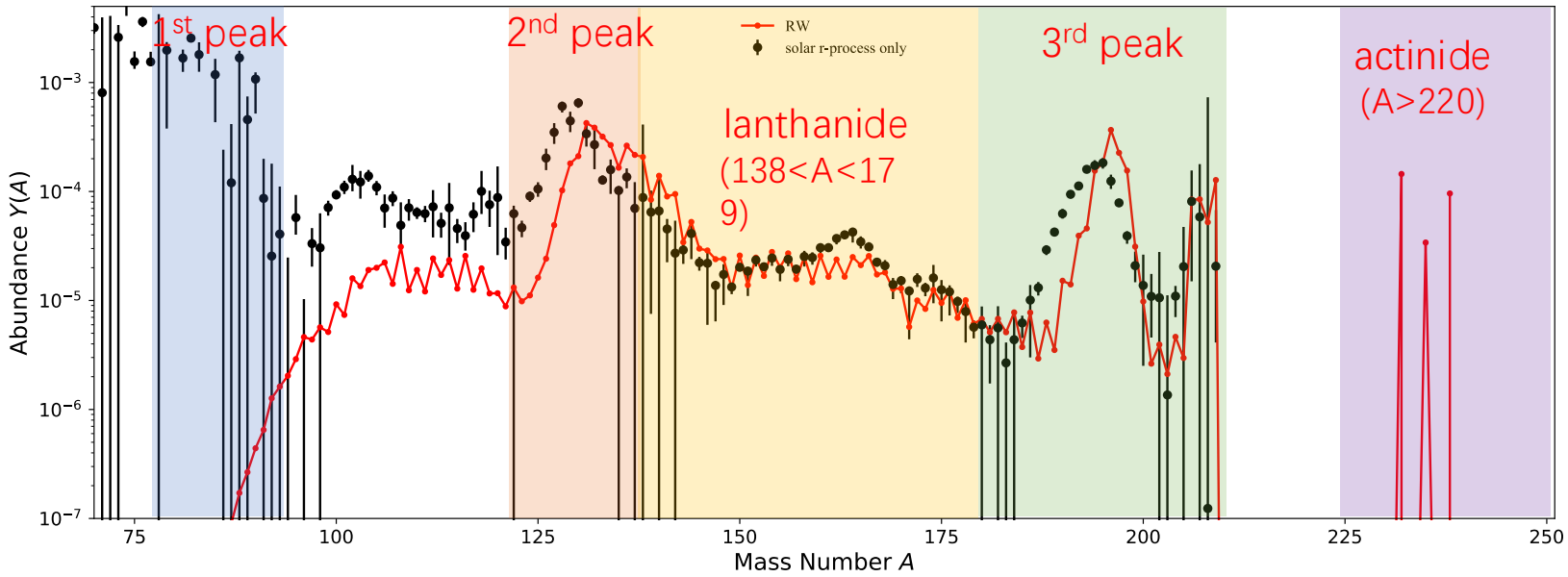
Koll, D., et al. 2026, Nature Astronomy, 10, 1001–1010

^{244}Pu: only made in r-process

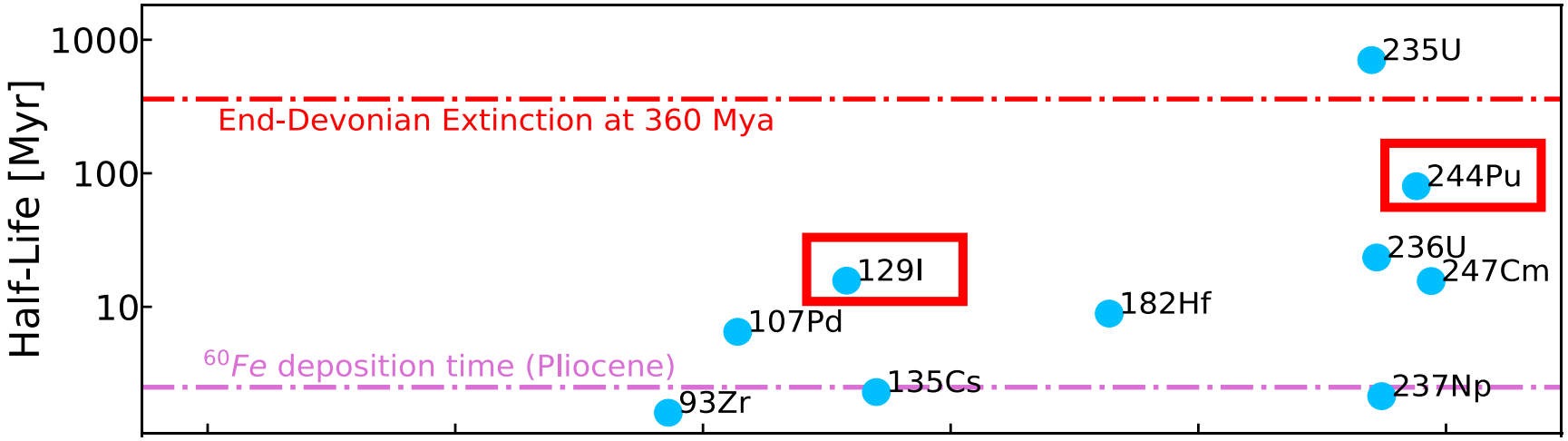
$t_{mean,^{244}_{94}\mathrm{Pu}} = 115\ Myr$

→ other long-lived r-process radioisotopes should also be present

Long lived r-process radioisotopes



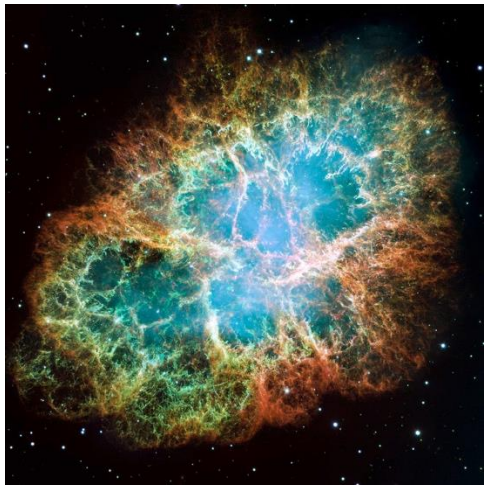
Isotopes with half-lives $t_{1/2}$ ~ 1 Myr to 1 Gyr



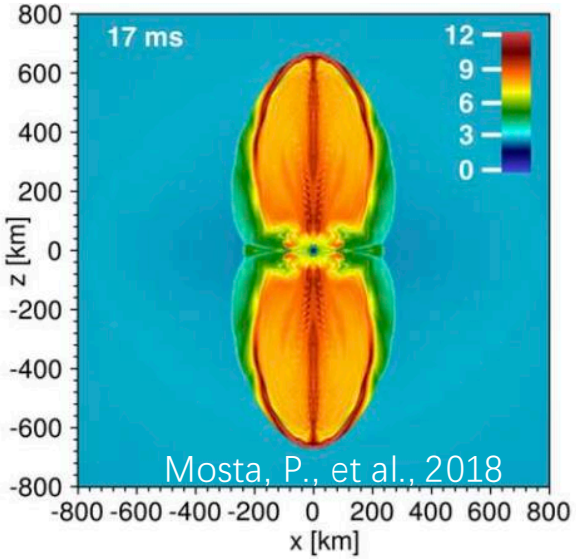
Wang, X., et al., 2021, ApJ 923, 219

r-process calculations

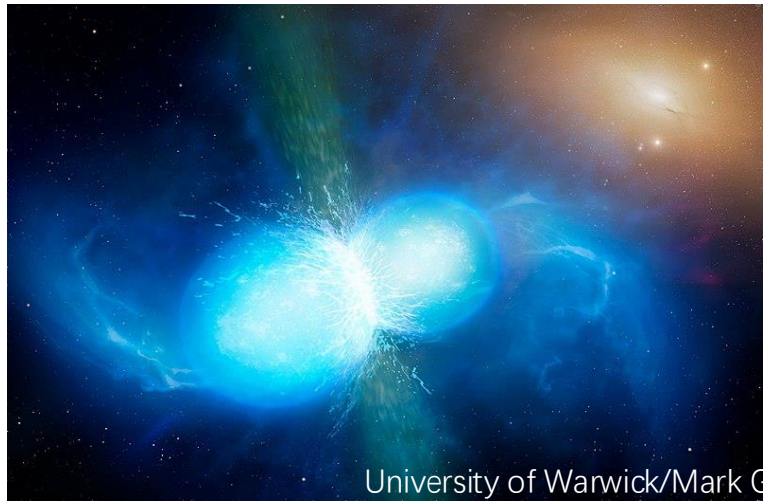
	Supernova (SN) Models		Kilonova (KN) Models	
Label	SA ($\nu\star$)	SB (MHD)	KA	KB
Simulations	SN *forced* neutrino-driven wind: 4 trajectories from Arcones et al. (2007); Arcones & Janka (2011b) with modified $Y_e = 0.31, 0.35, 0.42, 0.48$	MHD SN: 2 trajectories from Mösta et al. (2018b)	KN dynamical ejecta: 2 trajectories from Bovard et al. (2017) diskwind: 2 trajectories from Just et al. (2015)	
Scaling	HD160617: Yb, Te, Cd and Zr	HD160617: Yb and Zr	HD160617: Yb and Zr	J0954+5246: Yb and Zr
Mixing fractions f	$f_{0.35}$=0.757, $f_{0.42}$=1.778, $f_{0.48}$=0.770	3.137	3.980	0.819



Core collapse Supernovae



Magneto-rotational supernovae (MHD)



Neutron star mergers (kilonovae)

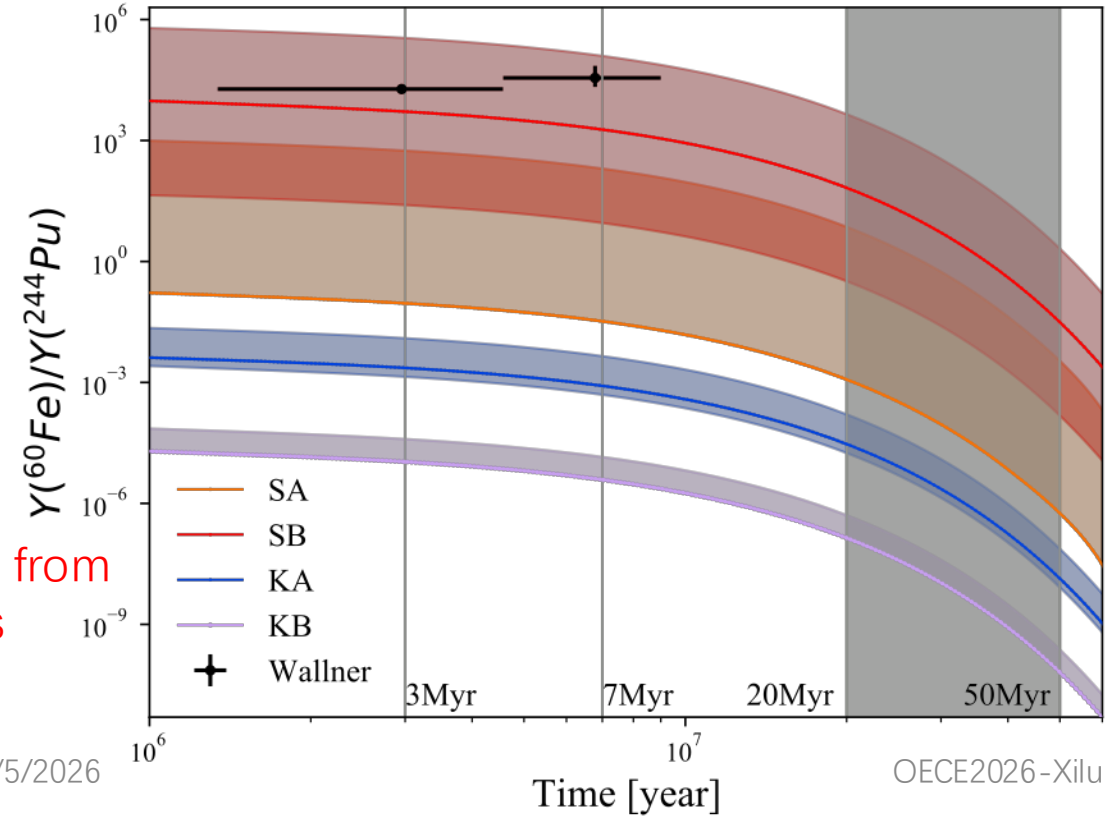
Nucleosynthesis simulation with PRISM

1) Baseline: AME2016 + FRDM2012 masses; Nubase2016 spontaneous fission and β decay rates; theoretical calculations from LANL (HF for n capture and n-induced fission; QRPA+HF for β-delayed fission and β-delayed neutron emission); symmetric split fission yields.

2) Variations: HFB masses (Goriely et al. 2009); β-decay rates from Marketin et al. (2016) (MKT); fission yields from Kodama & Takahashi (1975)

r-process calculations

	Supernova (SN) Models		Kilonova (KN) Models	
Label	SA ($\nu\star$)	SB (MHD)	KA	KB
Simulations	SN *forced* neutrino-driven wind: 4 trajectories from Arcones et al. (2007); Arcones & Janka (2011b) with modified $Y_e = 0.31, 0.35, 0.42, 0.48$	MHD SN: 2 trajectories from Mösta et al. (2018b)	KN dynamical ejecta: 2 trajectories from Bovard et al. (2017) diskwind: 2 trajectories from Just et al. (2015)	
Scaling	HD160617: Yb, Te, Cd and Zr	HD160617: Yb and Zr	HD160617: Yb and Zr	J0954+5246: Yb and Zr
Mixing fractions f	$f_{0.35}$=0.757, $f_{0.42}$=1.778, $f_{0.48}$=0.770	3.137	3.980	0.819



^{60}Fe only from r process

- SN: ^{60}Fe mostly comes from explosive nucleosynthesis and stellar burning → ^{60}Fe in r process production serve as a lower limit for SN models SA and SB
- For direct deposition, ^{60}Fe/^{244}Pu:
  - KN models fail
  - ”modified ” SN neutrino driven wind and MHD SN can work → must be rare SN

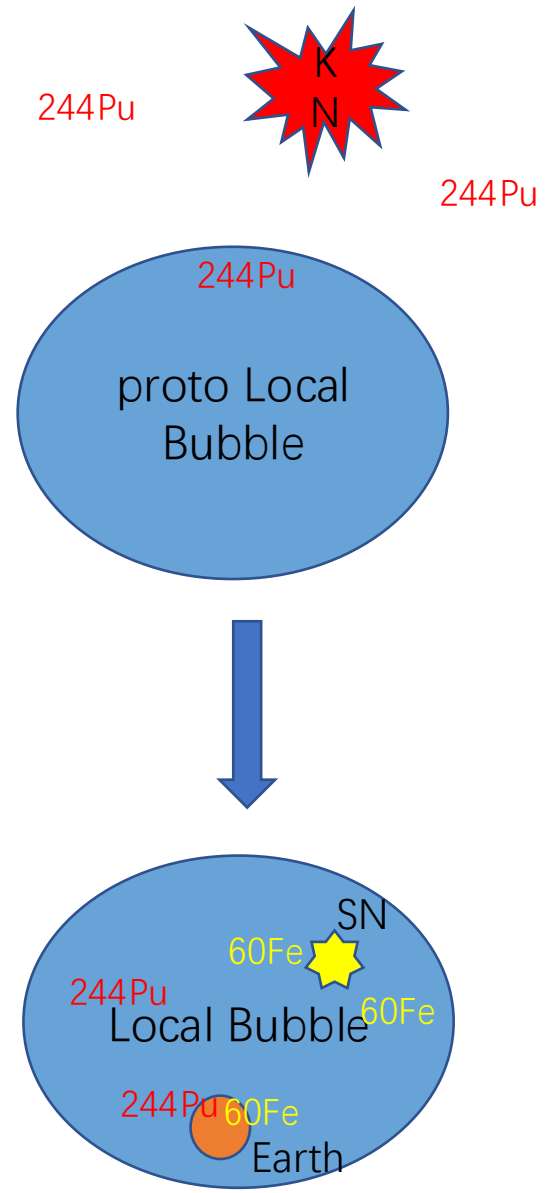
^{244}Pu: Two-Step Kilonova Scenario

Kilonovae/Neutron Star mergers:

- ➢ Robust r-process sites → ample ^{244}Pu productions
- ➢ Rare events
- ➢ Unlikely within Local Bubble

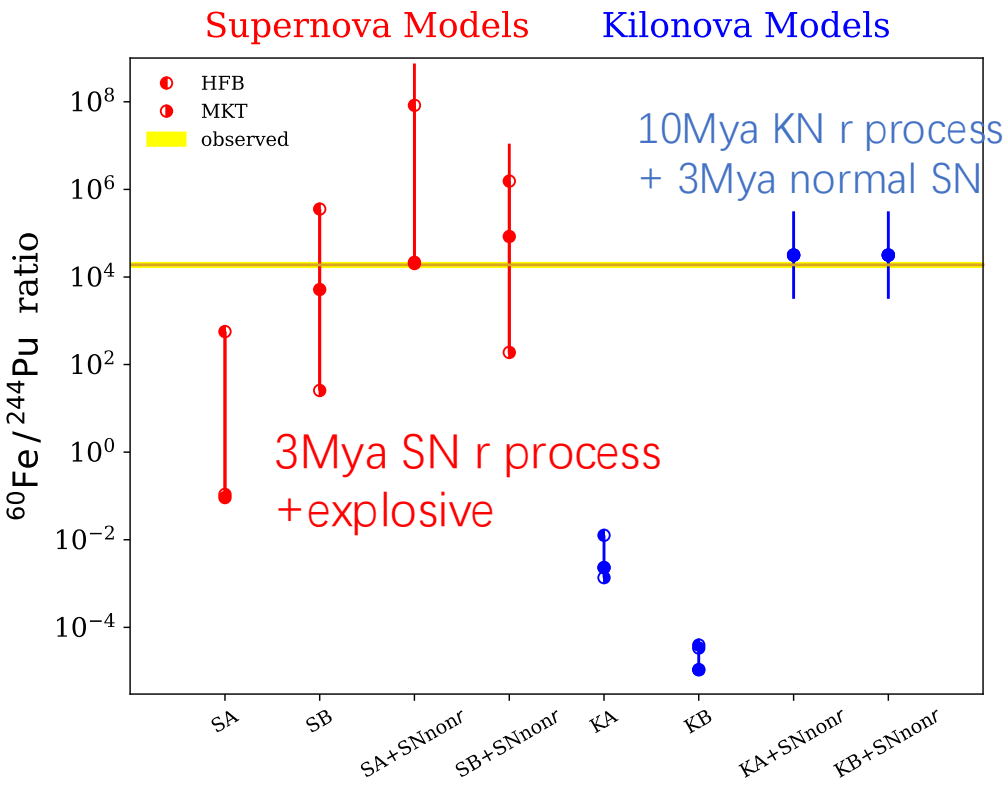
"Two-step" scenario for Kilonovae:

- ❖ More than~10-20 Mya, a KN exploded, ejecting ^{244}Pu-bearing r-process material
- ❖ Some of the KN ejecta collided with and was mixed into the molecular cloud giving rise to the Local Bubble
- ❖ Some of the ^{244}Pu was incorporated into dust grains, and a more recent SN swept the ^{244}Pu-bearing dust to bombard the Earth.



Wang, X., et al., 2021, ApJ 923, 219

^{244}Pu from Near-Earth Supernovae or Kilonovae



Wang, X., et al., 2023, ApJ 948, 113

- ^{60}Fe/^{244}Pu measurement :
  - Direct deposition: ”modified ” SN neutrino driven wind and MHD SN can work → must be rare SN
  - Two step KN scenario: 10Mya-50Mya KN + a normal non-r-process SN
- Tests: other long-lived r-process species ^{93}Zr, ^{129}I, ^{182}Hf….

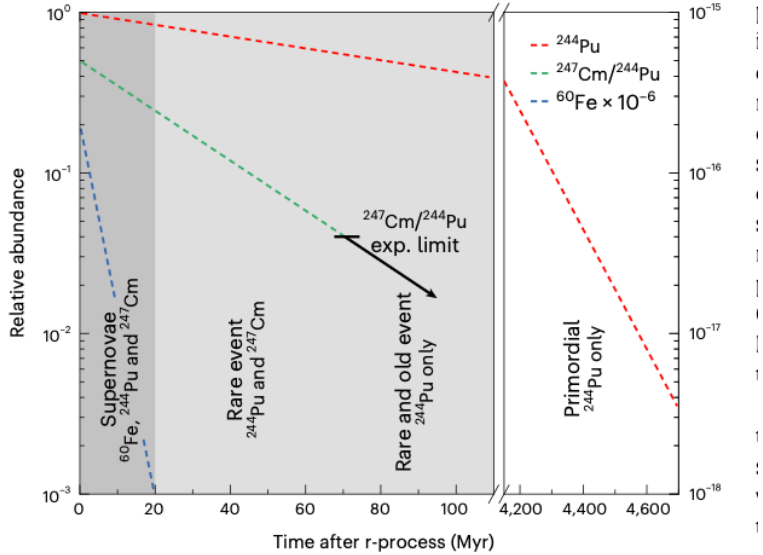


Fig. 2 | Radioactive decay curves of ^{60}Fe, ^{244}Pu and ^{247}Cm/^{244}Pu. A ^{247}Cm/^{244}Pu ratio of 0.5 is fixed after the r-process event and decreases purely through radioactive decay with an effective half-life of 19.3 Myr. The experimental ^{247}Cm/^{244}Pu limit of <0.04 in VA13/2-237KD represents a time limit for the last r-process event near Earth of >70 Myr ago. Considering a relative enrichment factor of 2.5 for Cm/Pu in VA13/2-237KD (Methods), the time limit becomes >95 Myr ago. Recent supernovae (dark grey area) and a recent rare event as r-process sites of the detected ^{244}Pu are excluded by the non-detection of ^{247}Cm, suggesting an old and rare event as the r-process site.

Koll, D., et al. 2026, Nature Astronomy, 10, 1001–1010

Non-detection of ^{247}Cm
→an old r-process event

Predictions for future measurement of the r-Process Radioisotopes

中国探月
CLEP

ARTEMIS

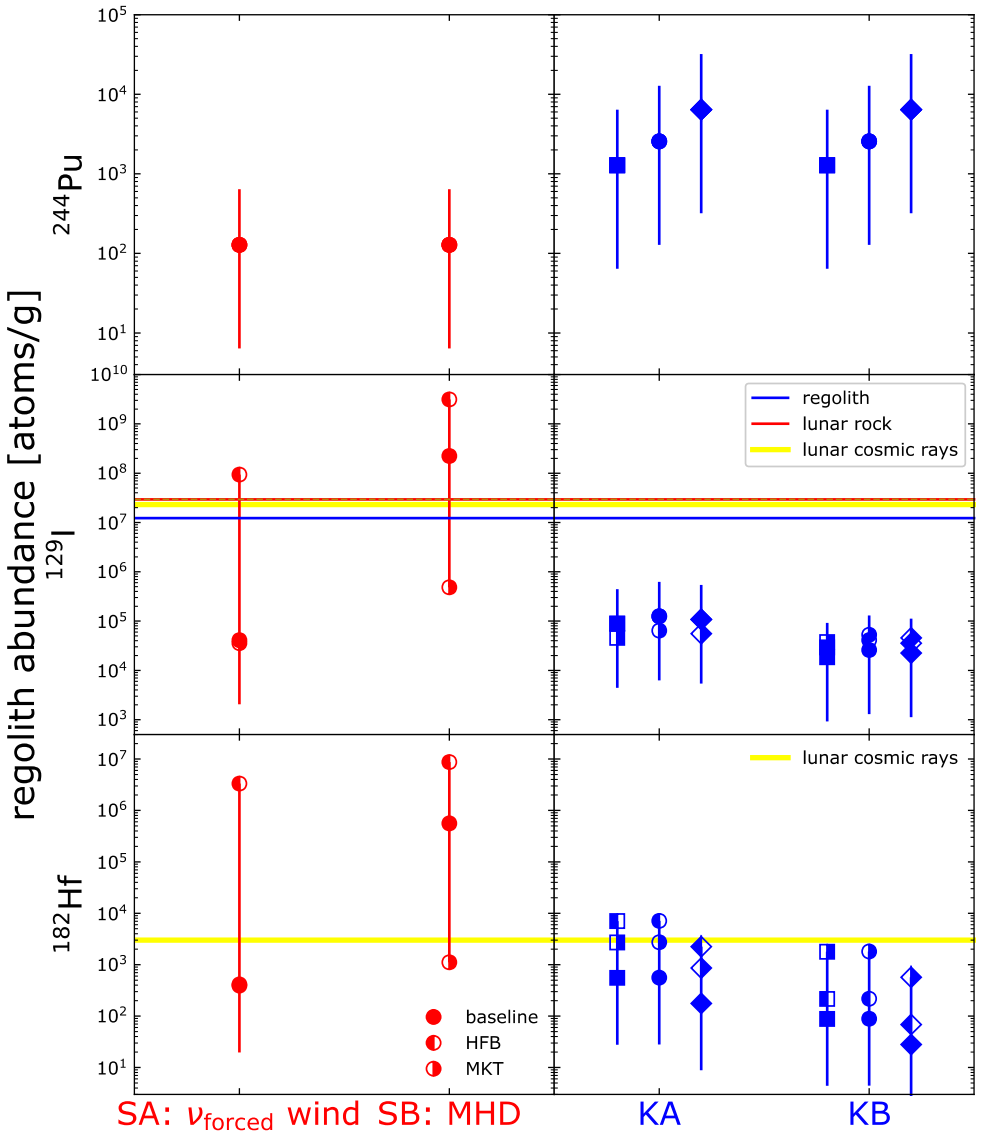
Lunar regolith samples

→ Avoid anthropogenic contamination

→ Future measurements of the samples from Chang'e and Artemis missions

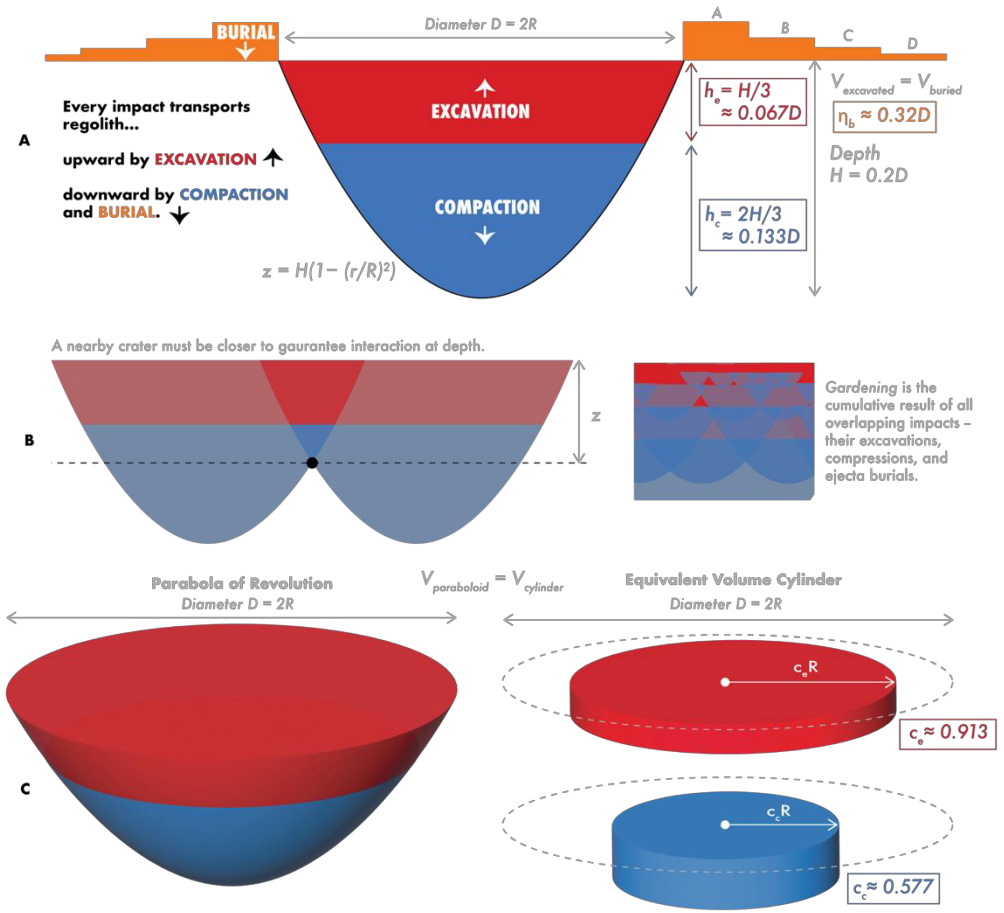
Table 2. Lunar Regolith *r*-Process Radioisotopes From Near-Earth Explosions

Isotope	Cosmic-Ray Targets	AMS Sensitivity [atoms]	Background [atoms/g]	Sample Mass [g] SN	KN
^{129}I	Te, Ba, La	10^5	10^7	$10^{-1} - 10^3$	1–10
^{182}Hf	^{183}W, ^{184}W, ^{186}W	10^7	3×10^3	$2 - 5 \times 10^5$	$3 \times 10^3 - 10^6$
^{244}Pu	–	10^2	–	10	



Wang, X., et al., 2023, ApJ 948, 113

New Lunar Gardening Model: Guide the Search for Supernova Debris in the Lunar Regolith



Lunar impacts redistribute regolith by excavating, compacting, and burying material. We present a mass-conservative analytic model of this transport efficiency with **the net vertical transport depth** as:

$$D_z(t) = D_B(t) + D_C(t) - D_E(t)$$

$$= \underbrace{\left[\eta_b(b) + \frac{h_c}{c_c^{-\frac{2}{b-2}}} - \frac{h_e}{c_e^{-\frac{2}{b-2}}}\right]}_{\text{Geometric Efficiency}} \underbrace{\left(\frac{\pi abt}{4(b-2)\lambda}\right)^{\frac{1}{b-2}}}_{\text{Probabilistic Frequency}}$$

The evolution of concentration or number density C(z,t) is obtained from the **Advection-Diffusion Equation (ADE):**

$$\frac{\partial C}{\partial t} = \frac{\partial}{\partial z}\left(\kappa(t)\frac{\partial C}{\partial z}\right) - v_z(t)\frac{\partial C}{\partial z} - \lambda_{\text{decay}}C + S(z,t)$$

Diffusion

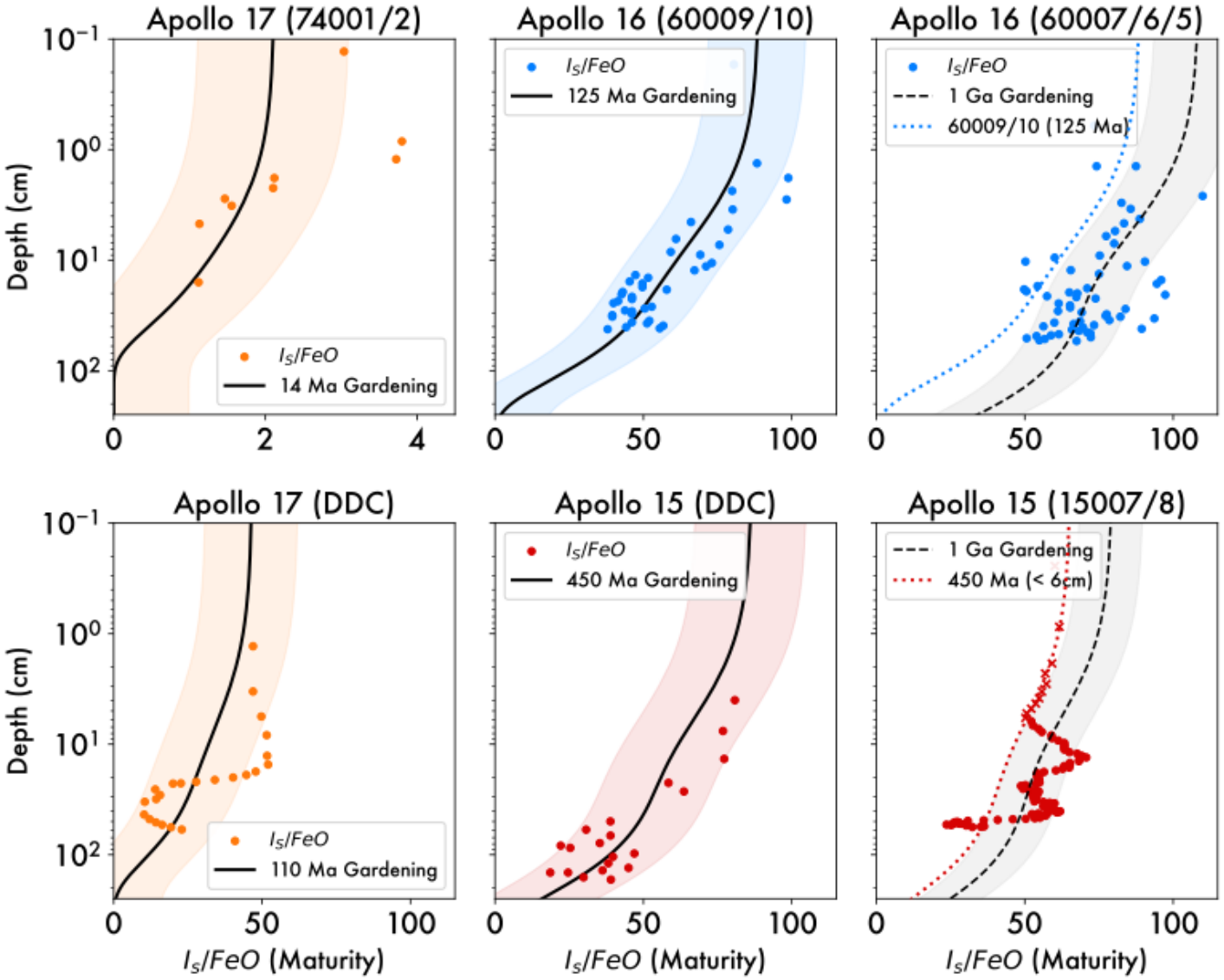
Advection $v_z = \frac{\partial D_z}{\partial t}$

S(z,t): the spatiotemporal source term

→continuous for maturity, episodic for supernova-derived ^{60}Fe, and continuous/depth-dependent for cosmogenic ^{60}Fe)

Costello, E., **…, Wang, X.**, 2026, PRL 137, 071005

New Lunar Gardening Model: Guide the Search for Supernova Debris in the Lunar Regolith

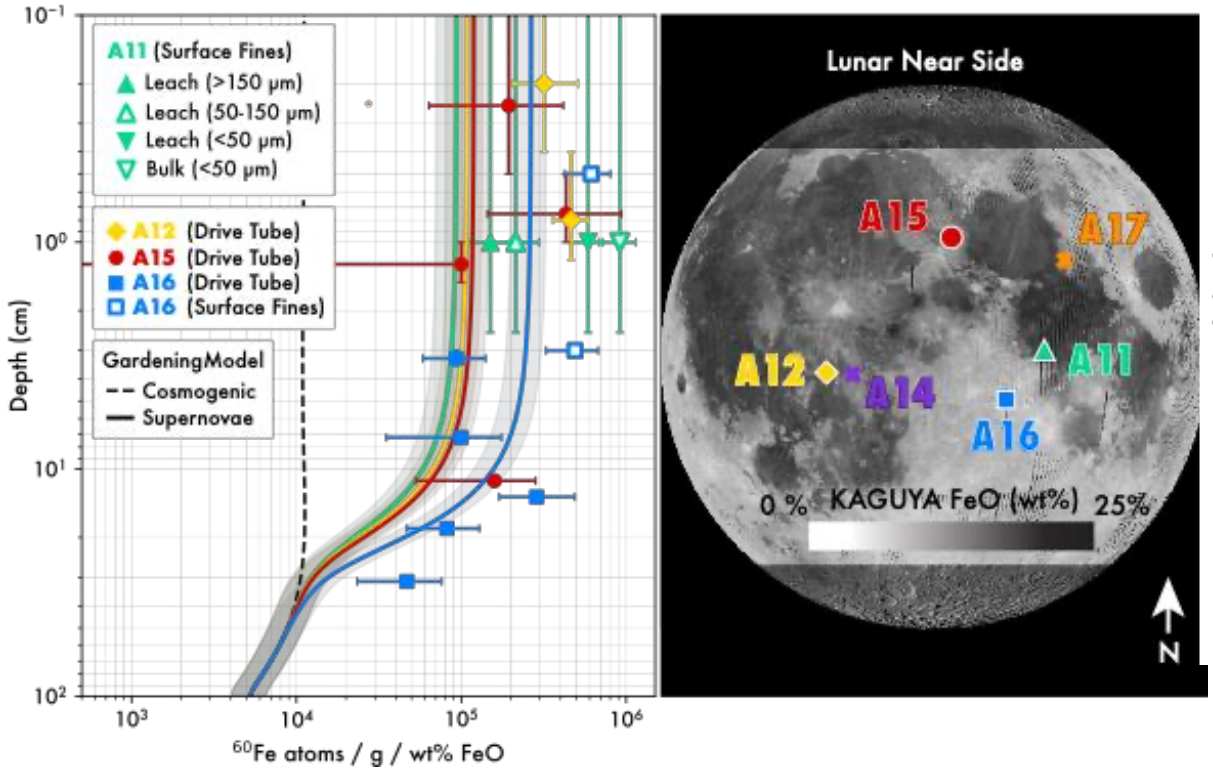


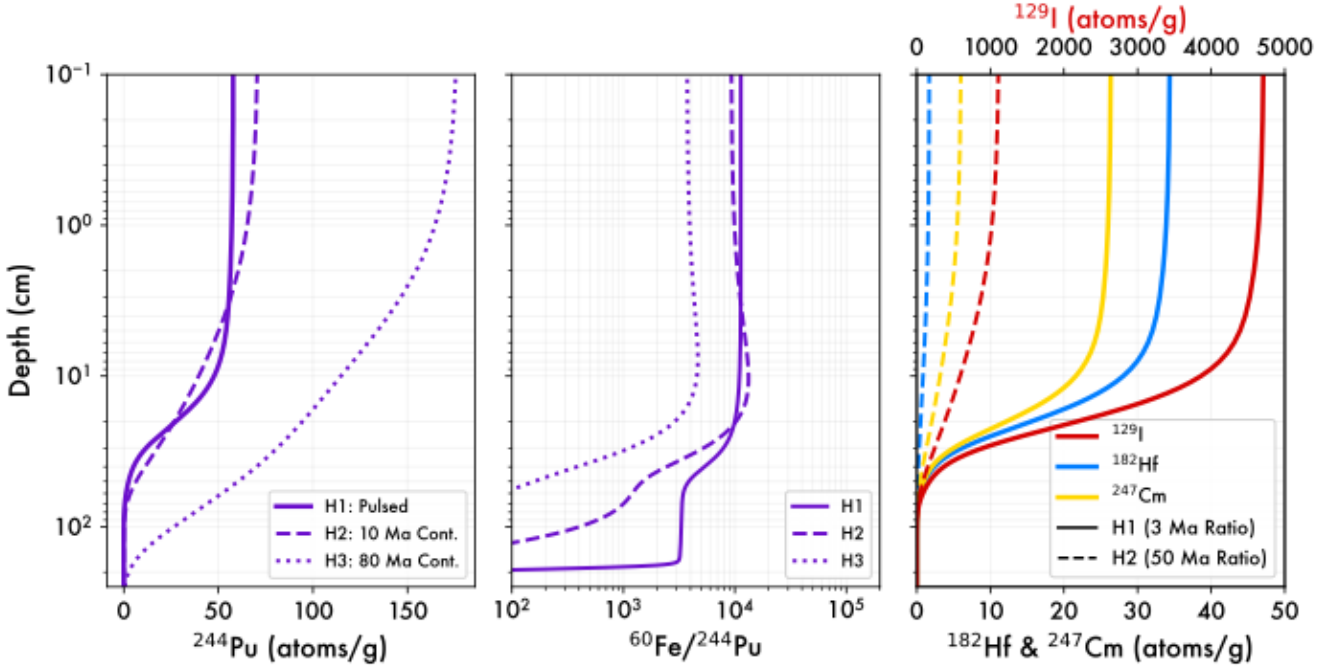
Validation: Regolith Maturity

→Surface maturity Is/FeO profiles for Apollo 15, 16, and 17 samples that validate the unified gardening model. The ages of these samples are independently constrained by cosmic ray tracks and radionuclide benchmarks

Costello, E., **…, Wang, X.**, 2026, PRL 137, 071005

New Lunar Gardening Model: Guide the Search for Supernova Debris in the Lunar Regolith





Solid line H1: 244Pu and r-process delivery is correlated with SN pulses centered at 2.3 Myr and 7.3 Myr

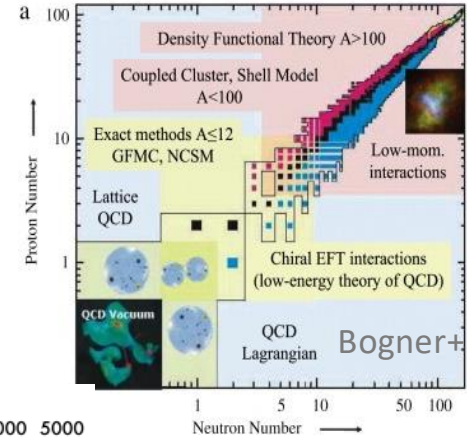
Dashed line H2: short-term continuous influx over the last 10 Myr with an injection time of 50 Myr

Dotted line H3: long-term continuous influx over the last 80 Myr

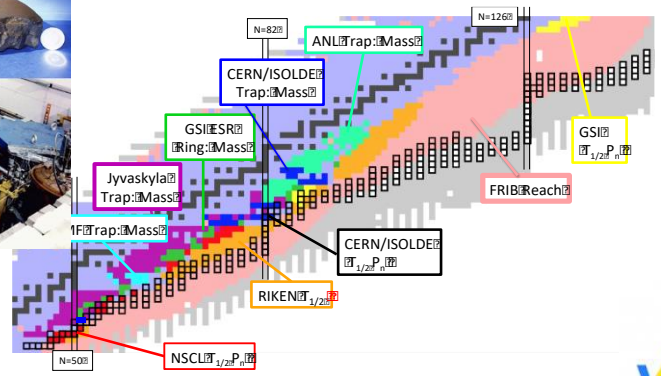
Costello, E., **…, Wang, X.**, 2026, PRL 137, 071005

Outlooks

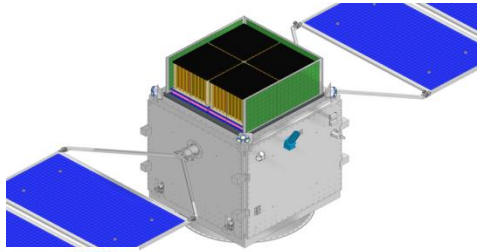
- What are the origins of the heaviest elements in our universe?
  - ➢Solution: Combination of theory, simulations, and experiments & observations

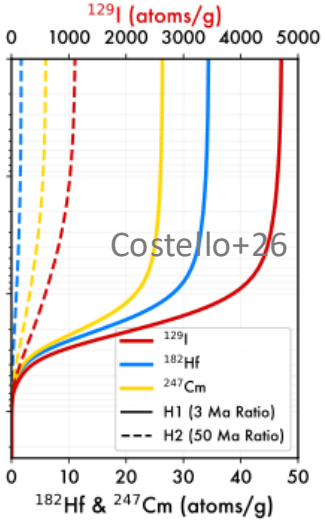


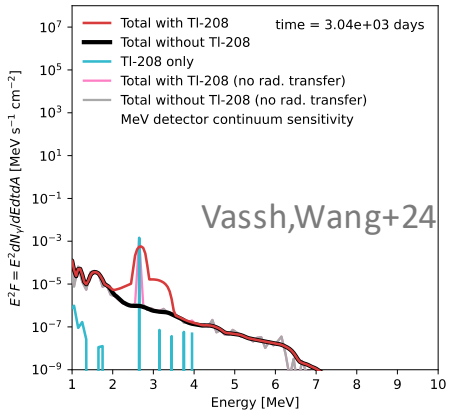


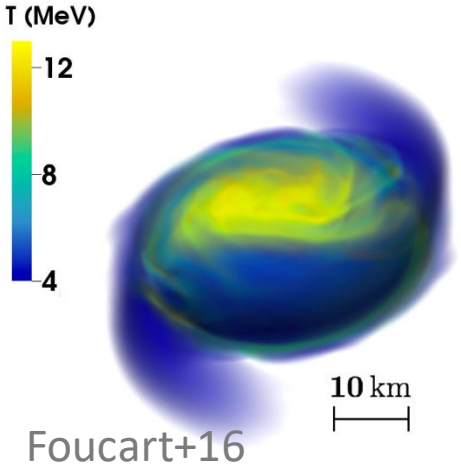


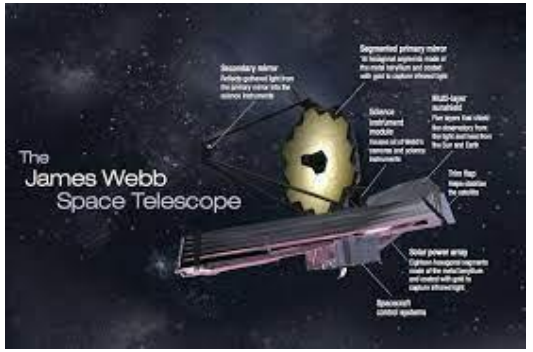
Horowitz+18













  - ➢A multi-disciplinary community working to illuminate heavy element origins
  - ➢r-Process radioisotopes are especially interesting to identify direct signals from individual astrophysical transients

- Thanks for your attention. Questions?